

THESIS FOR THE DEGREE OF DOCTOR OF PHILOSOPHY

**The construction, analysis and
validation of mechanistic
mathematical models of protein
kinetics in the context of replicative
ageing in budding yeast**

Johannes Borgqvist



UNIVERSITY OF GOTHENBURG

Division of Applied Mathematics and Statistics
Department of Mathematical Sciences
University of Gothenburg and Chalmers University of Technology
Gothenburg, Sweden 2020

The construction, analysis and validation of mechanistic mathematical models
of protein kinetics in the context of replicative ageing in budding yeast

Johannes Borgqvist

Gothenburg 2020

ISBN: 978-91-7833-910-5 (TRYCK)

ISBN: 978-91-7833-911-2 (PDF)

Available at: <http://hdl.handle.net/2077/64055>

© Johannes Borgqvist, 2020

Division of Applied Mathematics and Statistics

Department of Mathematical Sciences

University of Gothenburg and Chalmers University of Technology

SE-412 96 Gothenburg

Sweden

Telephone: +46 (0)31 772 1000

Cover image

Artist: Matilda Stävenborg

Caption: Mathematical modelling of protein kinetics in the baker's yeast
Saccharomyces cerevisiae in the context of ageing

Typeset with L^AT_EX

Printed by Stema Specialtryck AB, Borås, Sweden 2020

“Cela est bien, répondit Candide, mais il faut cultiver notre jardin.”

From “*Candide*” by Voltaire (1694-1778)

“We are going to die, and that makes us the lucky ones. Most people are never going to die because they are never going to be born. The potential people who could have been here in my place but who will in fact never see the light of day outnumber the sand grains of Arabia. Certainly those unborn ghosts include greater poets than Keats, scientists greater than Newton. We know this because the set of possible people allowed by our DNA so massively exceeds the set of actual people. In the teeth of these stupefying odds it is you and I, in our ordinariness, that are here. We privileged few, who won the lottery of birth against all odds, how dare we whine at our inevitable return to that prior state from which the vast majority have never stirred?”

From “*Unweaving the Rainbow: Science, Delusion and the Appetite for Wonder*” by Richard Dawkins (1941-)

The construction, analysis and validation of mechanistic mathematical models of protein kinetics in the context of replicative ageing in budding yeast

Johannes Borgqvist

Division of Applied Mathematics and Statistics
Department of Mathematical Sciences
University of Gothenburg and Chalmers University of Technology

Abstract

Mathematical modelling constitutes a forceful tool for elucidating properties of biological systems. Using theoretical approaches in combination with experimental techniques it is possible to study specific molecular aspects of phenomena such as the ageing of human beings. In fact, as many processes are similar in simpler organisms such as the budding yeast *Saccharomyces cerevisiae* it is possible to experimentally investigate for instance the accumulation of damaged proteins due to ageing in these biological systems. The aim of this thesis is to construct, analyse and validate mathematical mechanistic models of protein kinetics consisting of both ordinary and partial differential equations in the context of ageing. This is done both on a large time scale corresponding to the entire life span of cells and a short time scale corresponding to an isolated part of the cell division. The focus of the work on the large time scale is twofold, firstly the life span of individual yeast cells is modelled (Paper II) and secondly the life spans of vast numbers of cells in numerous populations are simulated (Paper III). Using a model of the accumulation of damage involving the forces cell growth, formation and repair of damage as well as the cell division, the impact of these individual parts on the overall fitness of individual cells and entire populations is investigated. On the short time scale, a more detailed model of a single protein called Cdc42 involved in the cell division is presented (Paper IV) and this theoretical framework has a high level of detail as it describes the spatial movement of the protein of interest within the cell over time. Given this precise description of the geometry of an individual cell, the mathematical properties of the model is analysed and these theoretical results are used to conduct numerical simulations of the activity of this protein. Lastly, an overall theme of the thesis is the difficulty of validating mechanistic models even in the presence of data. More precisely, as numerous and sometimes mutually exclusive models can describe a system equally well it is currently very hard,

even by calibrating the models to experimental data using statistical methods, to differentiate between various models. To this end, a mathematical tool called symmetry methods is introduced as a potential remedy to this problem, and using this methodology it is possible to extract information in the data as well as in the model that is not available using standard approaches. To showcase the power of symmetries, a minimal example of the usage of these methods in the context of enzyme kinetics is presented (Paper V). In conclusion, this work suggests that novel analytical tools such as symmetry methods could complement and assist the current standard approaches for modelling protein kinetics where the purpose is to deduce the underlying mechanisms of biological systems.

Keywords: Protein kinetics, replicative ageing, Cdc42, ordinary differential equations, reaction diffusion models, parameter estimation, model validation, model construction, symmetry methods.

Sammanfattning

Matematisk modellering utgör ett kraftfullt verktyg för att klargöra egenskaper hos biologiska system. Genom att använda teoretiska tillvägagångssätt kombinerat med experimentella tekniker så är det möjligt att studera specifika molekylära aspekter hos diverse fenomen såsom mänskligt åldrande. Faktum är att eftersom många processer är liknande i mer enkla organismer såsom den knoppande jästen *Saccharomyces cerevisiae* så är det möjligt att exempelvis undersöka ansamlandet av skadade proteiner till följd av åldrande i dessa biologiska system. Syftet med denna avhandling är att konstruera, analysera och validera matematiska mekanistiska modeller av proteinkinetik som består av både ordinära och partiella differentialekvationer inom ramen för åldrande. Detta görs både på en lång tidsskala vilket svarar mot hela levnadsspännet hos celler och en kort tidsskala svarande mot en isolerad del av celldelningen. På den långa tidsskalan så är arbetets inriktning tvådelat, för det första så modelleras hela levnadsspännet hos individuella jästceller (Artikel II) och för det andra så simuleras levnadsspännet hos ett ofantligt stort antal celler i flertalet populationer (Artikel III). Genom att använda en modell av ansamlande av skadade proteiner som innefattar krafterna celltillväxt, bildande och reparation av skadade proteiner samt celldelning, så kan effekten som dessa enskilda delar har på det övergripande välmåendet hos individuella celler och hela populationer undersökas. På den korta tidsskalan så presenteras en mer detaljerad modell av kinetiken hos ett enskilt protein vid namn Cdc42 som är inblandat i celldelningen (Artikel IV) och detta teoretiska ramverk har en hög grad av detalj då det beskriver den rumsliga rörelsen hos proteinet av intresse inom cellen över tid. Givet denna utförliga beskrivning av geometrin hos en enskild cell så analyseras de matematiska egenskaperna hos modellen och dessa teoretiska resultat används sedan för att genomföra numeriska simuleringar av aktiviteten hos detta protein. Slutligen så är ett övergripande tema i avhandlingen svårigheten att validera en mekanistisk modell även då data är tillgänglig. Närmare bestämt, då det ofta finns flertalet, ibland ömsesidigt uteslutande, modeller som kan beskriva ett system lika bra så är det i nuläget väldigt svårt, även genom att kalibrera modellerna till experimentell data med hjälp av statistiska metoder, att skilja olika modeller åt. För att potentiellt kunna åtgärda detta problem så kan potentiellt ett matematiskt verktyg vid namn symmetrimetoder införas och genom denna metodik så är det möjligt att utvinna information i både datan och modellen som inte är tillgänglig med hjälp av standardmetoder. För att visa upp förmågan hos symmetrier så presenteras ett testproblem då dessa metoder används inom ramen för enzymkinetik (Artikel V). Sammanfattningsvis, så visar detta arbete att nya analytiska verktyg såsom symmetrimetoder kan komplettera samt bistå de nuvarande standardmetoderna för att modellera proteinkinetik där syftet är att härleda de underliggande mekanismerna hos biologiska system.

List of publications

This thesis includes the following papers.

- Paper I **Borgqvist, J.**, Dainese, R., & Cvijovic, M. (2017), Systems Biology of Aging. *Systems Biology*, Wiley-VCH Verlag p243-264, doi: <https://doi.org/10.1002/9783527696130.ch9>
- Paper II **Borgqvist, J.**, Welkenhuysen, N. & Cvijovic, M.,(2020), Synergistic effects of repair, resilience and retention of damage determine the conditions for replicative ageing. *Scientific Reports*, 10(1):1556, 2020, doi: <https://doi.org/10.1038/s41598-020-58444-2>
- Paper III Schnitzer, B., **Borgqvist, J.** & Cvijovic, M. (2020) The Synergy of Damage Repair and Retention Promotes Rejuvenation and Prolongs Healthy Lifespans in Cell Lineages. (2020), *bioRxiv*, doi:<https://doi.org/10.1101/2020.03.24.005116> (*Submitted*).
- Paper IV **Borgqvist, J.**, Malik, A., Lundholm, C., Logg, A., Gerlee, P. & Cvijovic, M. (2020), Cell polarisation in a bulk-surface model can be driven by both classic and non-classic turing instability. *bioRxiv*, doi: <https://doi.org/10.1101/2020.01.29.925628> (*Submitted*).
- Paper V Ohlsson, F*, **Borgqvist, J.*** & Cvijovic, M. (2020), Symmetry structures in dynamic models of biochemical systems. *bioRxiv*, doi: <https://doi.org/10.1101/2020.01.27.922005> (*Submitted*). The "*" -symbol means that the first-authorship is shared.

Articles not included in the thesis

Welkenhuysen, N., **Borgqvist, J.**, Backman, M., Bendrioua, L., Goksör, M., Adiels, C. B., Cvijovic, M. & Hohmann, S. (2017), Single-cell study links metabolism with nutrient signaling and reveals sources of variability. *BMC Systems Biology*, 11(1), 59, doi: <https://doi.org/10.1186/s12918-017-0435-z>.

Author contributions

- Paper I I conducted a literature review and contributed substantially to the writing.
- Paper II I contributed significantly to the design of the project as well as with the majority of the ideas including the derivation of the model, derived the theoretical results, conducted all the programming, made all figures and did the majority of the writing.
- Paper III I contributed with some ideas and wrote the majority of the sections “introduction” and “discussion” of the article.
- Paper IV I designed the project, contributed with the majority of the ideas including the derivation of the model, took a substantial part in the derivation of the theoretical results, took a substantial part in the programming, made all figures and did the majority of the writing.
- Paper V I contributed substantially to the design of the project, contributed substantially with ideas, contributed substantially to the theoretical results, contributed substantially to the programming, contributed substantially to the figures and contributed substantially to the writing.

Acknowledgements

First and foremost, I would like to extend my sincerest gratitude and appreciation to my advisor Marija Cvijovic. Your never-ending encouragement has allowed me to take initiatives, it has instilled a great drive in me, it inspired me to listen to top class science at international conferences and it enabled me to pursue my various theoretical explorations into unknown mathematical territory while at the same time getting paid for it. Despite little sleep at points and stress at times, I have always been deeply enthusiastic since it has never been “just a job” for me. Or as some wise person once put it, “find your passion in life and you don’t have to work a single day”. Also, you have taught me invaluable lessons such as striking the right balance between life and work which has helped me to grow as a person tremendously. For this I am forever grateful, so thank you!

On top of this, I would also like to thank my second supervisor Fredrik Ohlsson. By pure coincidence you moved in to the same corridor around the time I started exploring symmetry methods, and it has been a great pleasure to delve into this mathematical field together with such an enthusiastic and esteemed scientist as you. In addition, I would like to thank my co-authors (Babsi, Niek, Adam, Carl, Philip, and Anders among others), it has been a pleasure to collaborate with other researchers with expertise in a variety of subject areas. Also, the research group of Cvijovic lab should be acknowledged as well as all the bachelor and master students that I have had the honour of supervising (I think I counted to 22 of you in total, so we could, theoretically, play a football match someday). On this point it is highly joyful that five of you now have started your own PhD journey where specifically two of you (Julia and Sebastian) are still in the group.

Also, I would like to thank the great people at the department of Mathematical Sciences and adjacent departments who I have gotten to know over these five short years. You are probably too many to name, but thank you to the lovely musicians in the infamous “Doktorandband”: Edvin, Henrik, Olof and Christian, thank you to the committee of the great(est?) workshop MBM: Felix and Filip, and I extend my gratitude to many more who I have encountered. To name a few: Oskar, Jonathan, Marco, Hung, Jacob, Anna, Sandra, Valentina, Milo, Linnea, Helga, Gabrijela, Sunney, Juan, Jiacheng, Mike, Malin, Caroline, Gustav, Per, Serik, Aila, Mohammad, Fardin, Axel, Annika and Martin.

Lastly, life is nothing without friends and family. So an acknowledgement to three groups of friends: “Elins vänner”, “Hisingspöjkarna” and “Les baGuettas” (merci pour les doigts magiques!). I am incredibly grateful for the support my wife Erica has provided me and for making my life so immensely meaningful. And to the little girl you are carrying, your father will be a “Doctor of Philosophy”, how about that?

Contents

1	Introduction	1
2	Background	5
2.1	Biology of ageing in the budding yeast	6
2.1.1	Formation of damage is a by-product of food uptake	8
2.1.2	To cope with accumulated damage the cell has developed systems for repairing and retaining damage	10
2.1.3	Cdc42-mediated cell polarisation in the context of ageing	12
2.1.4	Two experimental techniques for generating data of protein kinetics are microscopy and microfluidics	14
2.2	Mathematics of protein kinetics	16
2.2.1	Construction of kinetic models and non-dimensionalisation	19
2.2.2	Solutions of linear systems of ODEs and linear stability	22
2.2.3	Linear stability analysis of non-linear systems	24
2.2.4	Numerical methods for solving differential equations	27
2.2.5	Model validation, estimation of kinetic parameters (PE), numerical identifiability (NI) and selection of models	30
2.2.6	Symmetry methods for differential equations	36
2.2.7	Structural identifiability (SI)	48
3	Modelling of the entire life span of budding yeast	53

4	Modelling of Cdc42 mediated cell polarisation	59
5	Symmetries in the construction of mechanistic models	63
6	Summary of papers	69
6.1	Paper I - Systems Biology of Ageing	69
6.2	Paper II - Synergistic effects of repair, resilience and retention of damage determine the conditions for replicative ageing . . .	69
6.3	Paper III - Selective benefits of producing daughter cells of unequal reproductive potential in the population of a unicellular organism	70
6.4	Paper IV - Cell polarisation in a bulk-surface model can be driven by both classic and non-classic Turing instability	71
6.5	Paper V - Symmetry structures in dynamic models of biochemical systems.	72
7	Conclusions and outlook	73
8	Glossary of fundamental biological terms	77
	Bibliography	83
	Papers I, II, III, IV, V & VI	

List of Figures

1.1	Statistical versus mechanistic modelling	2
2.1	The budding yeast <i>Saccharomyces cerevisiae</i>	9
2.2	Workflow in systems and mathematical biology	19
2.3	An enzymatically catalysed reaction	20
2.4	Solutions to the ODE $du/d\tau = u/\tau$	37
2.5	The action of a symmetry	42
2.6	The relation between SI and NI	51
5.1	The blind men and the elephant	65
5.2	The vision of symmetries in mechanistic modelling	67

List of Tables

2.1	Example of experimental data in the form of a time series	31
3.1	Candidate models of damage accumulation	55
4.1	Candidate models of Cdc42-mediated cell polarisation	62

1 Introduction

In large parts of the world, illnesses related to ageing constitute a substantial problem. Medical conditions such as Huntington's, Parkinson's and Alzheimer's diseases impose severe problems on an individual and a societal level both in terms of suffering and financial costs. Thus, in the modern world it is of interest for the society as a whole to alleviate suffering by treating symptoms related to ageing and to this end an understanding of the phenomena is essential.

The deterioration of our bodies due to ageing is a consequence of the fact that reproduction is prioritised over longevity. As most animals in the wild die at a relatively young age on account of, for example, accidents, diseases or predation [68, 91] traits that correspond to rapid development allowing for fast reproduction are favoured by natural selection. Moreover, as animals have a limited amount of resources to spend on either maintenance of the body, called the *soma*, or on the germ cells, corresponding to investing in reproduction, processes related to the latter will be promoted rather than the former. Accordingly, higher organisms typically grow quickly in order to reproduce which is then followed by a quick degradation of the soma [77]. This is the essence of the so called *disposable soma theory* [55, 68, 91, 116, 118] which is the accepted evolutionary theory as to why ageing occurs. Due to the advancement of medical science, a larger number of human beings do not die from the previously listed reasons and thus ageing is a natural consequence of modern life. As ageing like most biological phenomena is highly complex it is often studied in simpler so called model organisms.

The baker's yeast *Saccharomyces cerevisiae* (*S. cerevisiae*) is an advantageous model organism for studying ageing. This is due to the fact that its biological foundation is highly similar to higher animals such as human beings, it is unicellular, it has a short life-span and it is extremely well-studied experimentally. Most importantly, it undergoes ageing as its cellular functions decline over time and as it shares many fundamental properties with human beings,

the biological details of specific illnesses such as Alzheimer's disease can be studied in yeast [8, 85, 89, 111]. Despite the relative simplicity of *S. cerevisiae*, its biology is still highly complex and governed by intricate reaction networks. Furthermore, as merely isolated parts of these biological systems can be observed experimentally, and as an understanding of the interaction of multiple unobserved components are required to elucidate the underlying mechanism of the studied system researchers often resort to mathematical modelling.

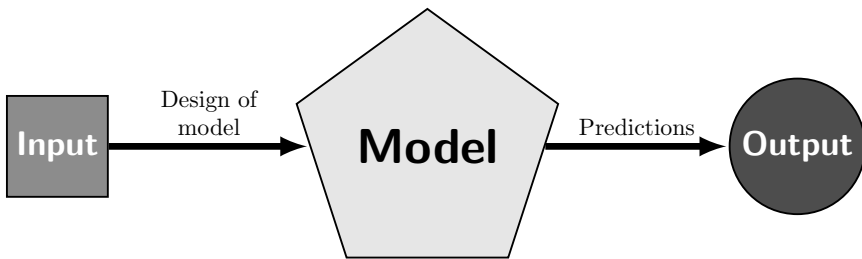


Figure 1.1: Statistical versus mechanistic modelling. Statistical modelling focuses on describing a set of outputs from a set of given inputs where the model itself is not necessarily of interest and it is often treated as a “black box”. To the contrary, in the context of mechanistic modelling the construction and structure of the model as well as its properties are emphasised.

A mechanistic model constitutes a theoretical holistic description of a complex biological system. Although only limited parts of a system can be studied experimentally, a model can connect numerous inaccessible components in a theoretical framework which enables the proposal of an underlying mechanism. In fact, the mechanism is built into the very structure of the proposed model and thus the validation of a mechanistic model implies the proposal of an underlying mechanism. Empirically, biological systems can be studied by altering a controllable input, such as the availability of food, and observing the response of some measurable output, e.g. the expression of a certain gene. Mechanistic models are validated by testing whether or not the proposed model can describe the measured data. It should be noted that so called statistical models generally aim at connecting an input to a certain output without analysing the, typically very simple, structure of the model in contrast to mechanistic models where the actual model is the focus (Fig 1.1). However, the difficulty of validating a mechanistic model is that multiple different and sometimes mutually exclusive descriptions can sometimes capture the available data equally well which obstructs the task of finding the correct mechanism.

The work presented in this thesis consists of the construction, validation and analysis of mechanistic models of ageing in the baker's yeast *Saccharomyces cerevisiae*. As multiple common features of human and yeast ageing involve proteins, the kinetic models in this work describe the change in concentration of age-related proteins over time and sometimes in space (i.e. specific locations in the cell). Furthermore, in this work the ageing of yeast is modelled on two different time-scales, namely a long time-scale corresponding to the entire life span of yeast cells (Chapter 3) and a short time scale focusing on a single protein involved in the cell division (Chapter 4). As a common theme in both these cases is the difficulty of deducing the mechanism corresponding to the construction of the *correct* model, we propose a potential remedy in a specific mathematical tool called *symmetry methods* (Chapter 5). Before all this, the biological and mathematical background is presented (Chapter 2).

2 Background

As mechanistic modelling requires knowledge in both biology and mathematics, the background is divided into two parts. Firstly, the biological theory behind ageing in the baker's yeast *S. cerevisiae* is described (section 2.1). Secondly, the mathematics related to mechanistic models of protein kinetics is presented (section 2.2).

It should be emphasised that one of the difficulties with interdisciplinary research is that knowledge in numerous fields is required. Therefore, both these sections focus on the theory necessary for understanding the crucial concepts in the subsequent chapters (Chapter 3-5). As my intention is that both theoreticians and experimentalists within the research field should be able to read the text, this chapter constitutes a condensed introductory course about the major topics of the thesis. The difficulty level of the biology section of the background assumes that terms such as DNA, RNA, and proteins are familiar and if not it is advised to read the glossary in Chapter 8 *before* proceeding with the background. The difficulty level of the mathematical section assumes elementary knowledge in analysis, differential equations, linear algebra, numerical analysis, optimisation and statistics. The last part of the mathematical background, i.e. subsection 2.2.6, about symmetry methods is perhaps of particular interest for the theoreticians since this topic is quite rarely used in mathematical biology and since it tackles differential equations from a perspective that is fairly novel in the field. Thus, to introduce this, perhaps, unfamiliar topic, quite a lengthy background has been provided here where it is assumed that the reader has no knowledge of the topic in advance.

Moreover, if the reader has a background in biology it is advised to skip the biology section and vice versa if the reader has a theoretical background with regards to the mathematical section. Lastly, if the reader is solely interested in the actual research it is advised to skip this entire chapter and jump to the subsequent ones.

2.1 Biology of ageing in the budding yeast

Since the disposable soma theory of ageing relies on multicellularity, it was long believed that unicellular organisms were immortal. Or to quote George C. Williams [118] who expressed this sentiment as follows

“The theory regards ageing as an evolved characteristic of the soma. We should find it wherever a soma has been evolved, but not elsewhere.”

The balance between maintaining the body, i.e. the soma, and reproducing corresponding to investing in the germ line is referred to as a *division of labour*. Since unicellular organisms such as the baker’s yeast *S. cerevisiae* lack a soma it implies by the original formulation of the evolutionary theory that unicellular ageing should not occur. In the presence of food, yeast cells grow until a certain size is reached and then they divide. This cell division which is called *budding* results in the generation of two cells, one larger mother cell and one smaller daughter cell, from one original cell (Fig 2.1B). However, with each division the mother cell becomes phenotypically older [1] (while the daughter cells remain young) which ultimately culminates in cell death [72] confirming that budding yeast undergoes ageing. In fact, a yeast cell can only undergo a finite number of divisions before cell death occurs [7], more precisely around 20-30 divisions [7, 48], and the number of divisions before cell death is called the *replicative life span (RLS)*. This constitutes one measure of the age of yeast cells in the presence of food, but it is also possible to quantify age by means of the chronological life span defined as the time to cell death in the absence of food. The focus of this thesis is replicative ageing¹ as it resembles the ageing process in human cells, and in fact the ageing of unicellular organisms is in accordance with the evolutionary theory of ageing. This is due to the fact that on a population level it is possible to argue that the division of labour occurs between the mother cells (analogous to the soma) and the daughter cells (analogous to the germ cells) [77]. We have yet to define what we mean by ageing except for loosely describing it as the gradual deterioration of cells, and to be able to construct a model of the process the specific characteristics of yeast ageing must be described.

Yeast ageing is characterised by a number of features. Examples of such properties are an increase in both generation time² and the size of the cell,

¹In fact, when the term “ageing” is used throughout this thesis it exclusively refers to replicative ageing.

²The generation time is the time it takes for cell division to occur.

an accumulation of bud scars³, mitochondrial fragmentation and perhaps most importantly an accumulation of so called *ageing factors* corresponding to “damage” [110]. There are numerous types of damage where certain are specific to yeast such as *Extra-Chromosomal rDNA Circles (ERCs)* [78, 101] and others are more universal. Of the latter type, three examples are malfunctioning mitochondria [47], the production of *reactive oxygen species (ROS)* [27, 60, 74] and the accumulation of damaged proteins [1, 25, 78, 97]. Specifically, the proteins Htt103Q involved in Huntington’s disease, β -Amyloid involved in Alzheimer’s disease and Alpha synuclein in Parkinson’s disease can all be studied in yeast [97]. Also, as proteins execute the majority of the functions of an organism as well as constituting the building blocks of the cells it is the corresponding ageing factor that is the focus of this work. Moreover, the basic make up of yeast cells is similar to animal cells which makes the budding yeast in particular an appropriate model organism for human ageing.

The budding yeast *S. cerevisiae* is a unicellular⁴ *eukaryote*. This means that it is of the same type as the cells in higher animals implying that aspects of human ageing, for example, can be studied in budding yeast and it is also one of the most well-studied eukaryotic systems. Specifically, as yeast cells are more primitive than higher animals the former type has evolved earlier than the latter. Thus, if a biological feature is common to both these systems it implies that it is important as it has been preserved throughout evolution and these properties are referred to as *evolutionary conserved*. Furthermore, unlike the smaller and even more primitive bacteria, eukaryotic cells are bigger, they have various compartments with specialised tasks called *organelles* (Fig 2.1) and the DNA of eukaryotes⁵ is kept separated from the rest of the cell in a membrane enclosed compartment called the *nucleus* [2]. Thus, if the content of bacteria is a disordered soup protected by a thick cell wall a eukaryotic cell is more like an ordered city with different buildings responsible for specific tasks. In fact, the evolutionary theory called the *endosymbiont hypothesis* states that eukaryotic cells evolved as *anaerobic*⁶ hunters which engulfed smaller bacteria that could make use of oxygen through respiration [2]. Subsequently, some of them co-evolved with the original cell and these specific bacteria later became organelles such as the chloroplasts in plants or the mitochondria⁷ in animal cells.

³Bud scars are marks on the cell membrane where the daughter cell grows out.

⁴A unicellular organism consists of a single cell.

⁵The nucleus is the key distinction between eukaryotes and bacteria. In fact, the word itself is Greek where “eu” means “well” or “truly” and “karyo” means “kernel” or “nucleus” [2].

⁶Anaerobic organisms require (or occur in) the absence of oxygen.

⁷Strong evidence in support of this theory is that both mitochondria and chloroplasts contain bacterial DNA. Interestingly enough, this is why human beings are more genetically related to their mothers than their fathers as they inherit the mitochondrial DNA of their mothers.

As we will see, the mitochondria is a key component of ageing in both yeast and human cells. This is on account of the fact that damage is formed as a by-product of the main task of this organelle namely to provide the cell with energy from food taken up from the environment. As a response to toxic by-products, yeast cells have evolved various cellular responses to cope with damage. Subsequently, in the following subsections, the details of the formation of damage is presented first before the mechanisms for coping with damage are elaborated upon. After this, the focus is narrowed down when a particular aspect of the cell division concerning the protein Cdc42 is presented. Lastly, a section on the experimental techniques used to generate data follows as a transition to the next section of the thesis about mathematical modelling.

2.1.1 Formation of damage is a by-product of food uptake

In environments with oxygen, eukaryotic cells harness energy from the consumed food. This task is accomplished by the mitochondria which produces energy in the form of *adenosine triphosphate (ATP)*⁸ from the oxidation of food molecules, e.g. sugars. Specifically, the organelle contains various enzymes in its membrane which breaks down fatty acids and pyruvate with the aid of oxygen later leading to the production of ATP where one of the end products (which is released as waste) is carbon dioxide CO₂. Chemically, this entails the transport of electrons along the membrane and this transport electron chain is called the *respiratory chain* [2]. This transfer of electrons can lead to the formation so called *radicals* which are molecules with an unpaired valence electron [5] and these are typically highly reactive. In the case of the mitochondria, a class of such molecules called ROS⁹ [74] is formed in the organelle and these molecules can damage¹⁰ other parts of the cell such as components of the mitochondria or even proteins.

The fact that oxidative damage caused by mitochondria contributes to ageing is the essence of the “mitochondrial theory of ageing” [37]. In accordance with this theory, it has been shown that a yeast mother cell contains more ROS in its mitochondria than its daughter [60] and interestingly enough the daughter cells are able to clear their corresponding ROS [27]. Also, the production of ROS results in damaged mitochondria and accordingly a sign of ageing in yeast is the accumulation of damaged mitochondria. Normally, the cell has a system

⁸In fact, the majority of the cells ATP is produced from the mitochondria [2].

⁹It should be noted that ROS is an umbrella term which encompasses a large set of molecules with different chemical properties [74]. Examples are superoxide, hydrogen peroxide, nitric oxide, peroxy nitrite, hypochlorous acid, singlet oxygen and the hydroxyl radical.

¹⁰By “damage” in the case of proteins, we mean for example that these molecules can alter the shape of proteins which is critical for their functionality.

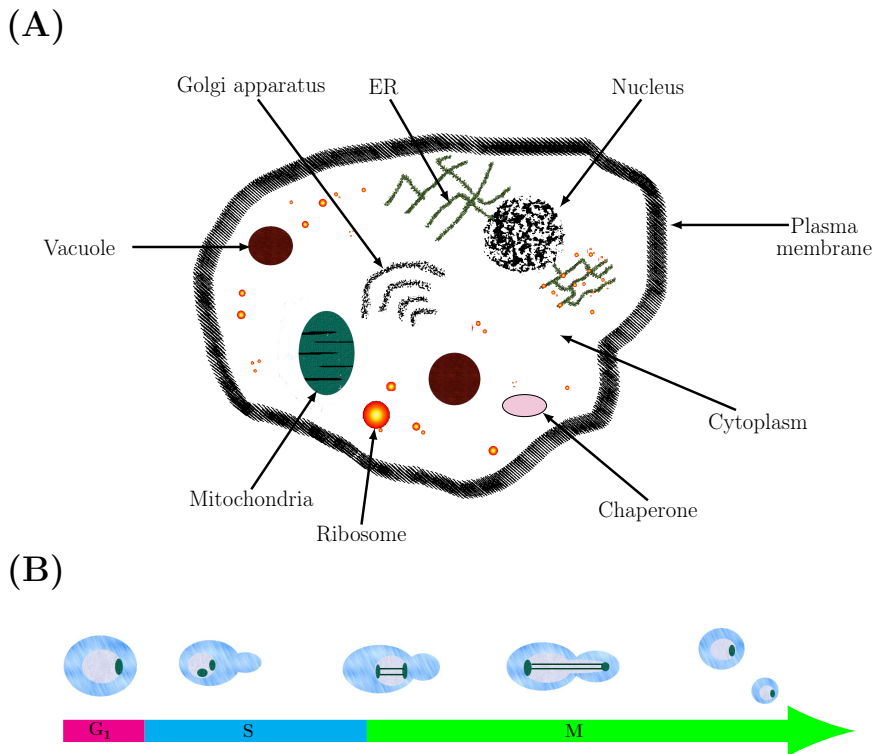


Figure 2.1: The budding yeast *S. cerevisiae*. (A): A schematic representation of the major organelles of the cell. The *nucleus* contains the DNA encoding the genetic information. The *plasma membrane* marks the boundary between the exterior and interior of the cell where the *cytoplasm* corresponds to the interior of the cell excluding the nucleus. The *chaperones* are proteins that promote the avoidance of the misfolding of other proteins as well as promoting the correct folding. The *ribosomes* are particles that translates RNA (specifically mRNA) into proteins. The *mitochondria* are the membrane-bound organelles conducting oxidative phosphorylation which produces the molecule ATP corresponding to energy that the cell can use. The *vacuoles* (called lysosomes in most animal cells) which are also membrane-bound degrade various molecules such as damaged proteins and they contain digestive enzymes to achieve this task. The *Golgi apparatus* is an organelle with a complex structure which sorts and modifies proteins and lipids from the ER (described next). The *Endoplasmic reticulum (ER)* is a membrane-bound organelle with a labyrinth-like structure which synthesises lipids and makes various proteins. The contents of the cytoplasm excluding the ER and the mitochondria is called the *cytosol*. (B): The cell cycle in budding yeast resulting in the generation of two cells, one large *mother cell* and one small *daughter cell*, from an original cell. The first phase corresponds to the G_1 -phase which is a gap-phase to allow the cell to grow and increase in mass. Budding yeast is special as it only has one gap phase while most other eukaryotes have an additional gap phase between the S- and M-phase called G_2 . The *S phase* is the phase where chromosome duplication occurs implying the synthesis of new DNA (note that the S-phase comprises half of the cell cycle in length implying that the arrow is not scaled). The *M phase* is where the chromosome segregation occurs which is divided into two events, nuclear division called *mitosis* and cytoplasmic division called *cytokinesis*. This sub figure is re-drawn based on Figure 17-5 in [2].

called *mitophagy* [47] which removes damaged mitochondria but as the cell ages the capacity to maintain mitophagy declines which is the cause behind this symptom of ageing. Moreover, mitochondria is not only crucial for ageing in yeast but it is also a determining factor in multiple aspects of human ageing. For example, in skeletal and muscle tissue the respiratory capacity of mitochondria decreases by 50% with age leading to a decline in production of ATP [29, 93]. Specifically this leads to a decrease in muscle strength which is believed to be the causal factor of age-related sarcopenia [82]. Another example is that dysfunctional mitochondria is closely connected to neurological disorders such as Alzheimer's and Parkinson's disease [110]. Hence, the production of ROS leading to the accumulation of damaged mitochondria is consequential for ageing.

In addition, the age-related ROS result in the production of oxidatively damaged proteins [1, 25, 110]. However, it should be emphasised that the exact extent to which ROS contribute to the formation of damaged proteins is not clear as the term constitutes numerous toxic oxygen species, and an increase in ROS does not always lead to a proportional increase in damaged proteins [74]. Besides, since the mitochondria is a very old organelle, various reactions in eukaryotic cells rely on ROS implying that these molecules are not always harmful but, in fact, necessary for the cell to a certain extent [74]. Further, as the formation of damage is a consequence of the activity of mitochondria it is logical to hypothesise that lowering the intake of food would promote longevity. This is exactly the idea of what is called *caloric restriction (CR)* which is a very well-studied life-prolonging strategy. For instance, it has been shown that CR increases the life span of yeast in low levels of glucose [63] and in fact this generalises to higher eukaryotes [36]. Nevertheless, despite this life prolonging strategy the inevitable formation of damaged proteins is a consequence of the uptake of food and to counteract these toxic components the cell has evolved specific systems.

2.1.2 To cope with accumulated damage the cell has developed systems for repairing and retaining damage

The *protein quality control (PQC)* system ensures that the available proteins are produced, renewed and that they function properly [38, 52]. This system is further divided into two parts, namely temporal and spatial PQC. The temporal PQC ensures the correct timing of the production of various proteins as well as focusing on repairing and degrading damaged proteins. The repair of proteins is conducted by a special class of proteins called (*molecular*) *chaperones* [2] which encounters newly synthesised proteins in proximity of the ribosomes. The

chaperones are crucial in assuring the function of proteins as they ensure the correct structure of proteins which is necessary for functionality. A big class of chaperones is the *heat shock proteins (Hsp)*¹¹ where Hsp70 [2] and Hsp40 [52] constitute a system which folds newly translated peptides. Another heat shock protein called Hsp104 which belongs to the class *disaggregases* can repair aggregated proteins by supplying the various peptides of the aggregate to the Hsp70-Hsp40 system [52]. Additionally, the proteins that cannot be repaired are degraded by the vacuole¹² which is a membrane-enclosed organelle containing digestive enzymes that can break down large macromolecules. Nevertheless, as the formation of damage increases with age the systems involved in temporal PQC cannot repair and degrade all of the damaged proteins. Consequently, ageing entails the accumulation of damage and to ensure that a young damage-free daughter cell is formed after cell division the mother cell retains most of the damage. In other words, the mother cell sacrifices herself by acting as a “rubbish bin” [78] at cell division by preventing the damage from leaking over to the daughter cells.

The systems involved in spatial PQC is responsible for the retention of damage in the mother cell. Initially, it was hypothesised that this retention was established merely by passive processes [122] such as the slow diffusion of the aggregates in combination with the fact that the size of the bud neck is very small. This entirely passive retention would imply that the cell division is completed before the aggregates manage to enter the daughter cell. However, it has since been demonstrated that the spatial segregation of damaged proteins at cell division has an active component (which is probably more influential) composed of at least two different systems.

The active retention of damage is based on protein inclusions and actin combined with the polarisome [77]. Smaller misfolded proteins are disposed into two different compartments called JUNQ (juxtannuclear inclusions) and IPOD (perivacuolar inclusions) [102] in the mother cell. Larger assemblies of damaged proteins organised into aggregates are rather retained using actin cables¹³ [77]. During cell division when the new cell grows out from the original cell, there are sites located at the tip of the daughter cell called the *polarisome* where actin filaments are synthesised [78]. The abundant protein actin forms large cable-like structures that connects both the mother and the soon to be daughter cell by binding to the cell membrane [2]. One can imagine the actin filaments

¹¹The heat shock proteins are named after the fact that their synthesis is increased spectacularly when cells are exposed to an increased temperature for a brief time [2]. This occurs as a response to the increased production of misfolded proteins due to the sudden rise in temperature.

¹²The vacuole is called the lysosome in higher eukaryotic cells [2].

¹³At least, this is the case in the context of Huntington’s disease [65].

being connected so as to form a large system of funicular railways¹⁴ along which the cell can retroactively transport aggregates from the daughter to the mother cell [65]. Two key disaggregases that are linked to the actin-based spatial PQC are the previously mentioned Hsp104 [64, 106] and a protein called Sir2 [1, 26, 80, 92]. Lastly, another key player in spatial PQC is the adaptor protein Vac17 involved in vacuole inheritance [115]. Vac17 generates inclusions for aged cells as well as limiting the inheritance of aggregates [39].

In summary, the biological processes involved in the retention of damage during cell division constitute a vital part of ageing in yeast as well as in higher organisms. Consequently, it is perhaps not surprising that other proteins involved in the cell division such as the master regulator *cell division control protein 42 homolog* (*Cdc42*) also play a role in the ageing of most eukaryotic organisms.

2.1.3 Cdc42-mediated cell polarisation in the context of ageing

Cdc42 is a highly evolutionary conserved *enzyme*¹⁵ in eukaryotic cells. More precisely, the importance (indicated by its evolutionary conservation) of this protein is affirmed by the fact that the Cdc42 of yeast is 80% similar to that of human cells [9, 12, 14, 22, 51, 66, 70, 73, 100]. The role of Cdc42 is that in the late G₁-phase it accumulates at a specific spatial location on the cell membrane, called the *pole*, which subsequently determines where the new cell grows out during cell division [10]. Moreover, it has been shown that the activity of Cdc42 is involved in both the ageing and the rejuvenation of hematopoietic stem cells [28, 30] in human beings. In addition, the Cdc42 pathway loses its function in aged yeast cells which in turn prevents replicative ageing [69]. Thus, to study the function of Cdc42 is of interest in the context of ageing in eukaryotic organisms in general and replicative ageing in yeast in particular.

The class of enzymes called GTPases to which Cdc42 belongs is an example of *molecular switches* [2]. In the cell, energy is often stored in terms of a molecule consisting of a *nucleoside* (which is a nitrogen base in the building blocks of DNA) bound to a number of phosphate groups. One such “energy storing”-molecule is based on the nucleoside *guanosine* and when this base is bound to three phosphate groups it is called *guanosine triphosphate* (*GTP*). Likewise, if it is bound to two phosphate groups it is called *guanosine diphosphate* (*GDP*) and the addition of a phosphate group resulting in the transition from GDP to GTP corresponds to the release of energy. Now, a *GTPase* is an enzyme

¹⁴For explanatory schematic figures of both systems of PQC, see [38, 77, 78].

¹⁵An enzyme is a protein that catalyses reactions in the cell, i.e. it aids the reaction to occur, without being consumed itself.

that is regulated by a molecular switch using GDP and GTP. More precisely, a GTPase is active when it is bound to GTP and inactive when it is bound to GDP. Moreover, the activation of GTPases relies on so called *guanine nucleotide exchange factors* (GEFs) and the inactivation relies on so called *GTPase-activating proteins* (GAPs). Also, it is possible to classify GTPases based on the events which precedes activation.

There are two families of GTPases which rely on signals from cell-surface receptors, namely the RAS and the RHO families [2]. Together with Rho and Rac, Cdc42 is one of the most well-studied members of the RHO family. As for all GTPases, Cdc42 is activated by GEFs and inactivated by GAPs and an astonishing fact is that there are more than 60 Rho-GEFs and 70 Rho-GAPs in humans [2]. A particular property of the GTPases of the Rho family is that it is the cell surface receptors that activate these enzymes by activating the corresponding GEFs, although the mechanisms behind the interaction between the cell surface receptors and the GEFs are, in most cases, unknown. Another characteristic of the Rho GTPases is that in the cytosol they are often bound to a so called *guanine nucleotide dissociation inhibitor* (GDI) [2] which prevents interaction with their corresponding GEFs, and a consequence of the binding of GDI to Cdc42 specifically is that it enhances mobility of the inactive GDP-bound form of the GTPase in the cytosol [14]. At the cell membrane, the active GTP-bound form of Cdc42, unlike the inactive form, can bind to various other proteins called *effectors* which further quickens the local activation of Cdc42 in a positive feedback loop [14].

The activation of Cdc42 is accelerated in a positive feedback circuit by two classes of effector proteins. Firstly, GTP-bound Cdc42 can bind to a so called *p21-Activated Kinases* (PAKs) which further can bind to a so called polarity scaffold protein [14]. The scaffold proteins, which are called Bem1 in the budding yeast *S.cerevisiae* and Scd2 in the fission yeast *Schizosaccharomyces pombe* (*S.pombe*), can then link the PAKs to the GEFs which can further activate Cdc42. Thus, the membrane bound effectors activates Cdc42 in a positive feedback loop as they recruit more GEFs to a site already containing active Cdc42. It is this sequence of events in combination with the fact that the different states of Cdc42 have varying rates of diffusion which underlie the polarisation process.

As mentioned before, the mechanisms behind the interaction between the effectors and regulators of Cdc42 are unknown. This is partly due to the fact that it is hard to measure these rates since the concentration of Cdc42 varies at different spatial locations on the cell membrane. Since the concentration profile of Cdc42 is inhomogeneous, it is essential to account for spatial effects when this protein is studied. Thus, a complication with studying the detailed properties of Cdc42-mediated cell polarisation experimentally is that high resolution spatial

microscopy is required. To account for this difficulty in order to elucidate the underlying phenomena, researchers often resort to mathematical modelling which is described in the next section. Before proceeding with the theoretical aspects of the background, a summary of the experimental techniques used for generating data will be presented subsequently.

2.1.4 Two experimental techniques for generating data of protein kinetics are microscopy and microfluidics

The experimental data used to validate models of protein kinetics is usually a time series. This is a table of the protein abundance, proportional to the concentration, at specific time points and it is usually generated through image analysis of microscopy images taken at each time point in the time series. In the specific context of protein kinetics, so called *fluorescence microscopy* is often implemented to detect particular proteins and there are two major techniques for render specific protein visible under the microscope. The first is to stain the proteins with *fluorescent dyes* [2] which are chemical compounds re-emitting light after being excited. An example of such a dye is *fluorescein* which emits green fluorescence as a response to being excited with blue light [2], and usually the dyes are coupled to antibodies that can bind selectively to a targeted protein [2].

The second technique is to insert genes encoding for so called *fluorescent proteins* [2]. These proteins are usually encoded by a single gene and the advantage of this technique is that by inserting a gene for these specific proteins the organism produces its own fluorescent molecules which can be detected as oppose to introducing foreign molecules to achieve the same result. Typically, these molecules are used as reporter molecules which entails that the gene of the fluorescent protein is inserted adjacent to the target protein, and in this way every time the target protein is expressed so is the fluorescent protein. However, a more specific usage of these molecules is to directly fuse the domain of the fluorescent protein with the target in order to create a fusion protein having the same function as the original target but at the same time being fluorescent. The most common of these proteins which was originally isolated from the jellyfish *Aequoria victoria* is called *green fluorescent protein (GFP)* but there are more similar alternatives such as RFP and YFP. It is the strength of the signal of the fluorescent light that is reported in the time series and usually a spatial average of the signal in a particular compartment of the cell, such as the nucleus, is calculated. Here, the strength of the signal is proportional to the concentration of the fluorescent protein. The staining of a specific protein or the creation of a particular fusion protein in order to study its kinetics is

typically done by altering the genetic code of the host organism, e.g. the yeast cell.

The insertion of a particular piece of DNA encoding a fluorescently tagged protein is enabled through *plasmid vectors* [2]. This is a circular piece of bacterial DNA that is readily taken up by microorganisms and here the methodology for staining proteins makes use of the efficient system that bacteria has evolved to interchange genetic information. Typically, the technique for inserting DNA into a plasmid revolves around two types of enzymes, namely *restriction nucleases* and *DNA ligases* [2]. The former class of enzymes corresponds to nature's "scissors" which can cut open a plasmid and the latter class facilitates the joining of DNA strands. In particular, this implies that the ligases can mend the broken plasmid while simultaneously inserting the piece of DNA encoding the fluorescent dye. In this way, cells that are *transfected*, i.e. that take up, the plasmid will express the fluorescent protein. Typically, the number of plasmids are immensely increased by introducing them into rapidly reproducing bacteria and in order to purify the liquid sample in which the colony is cultured so that it contain large quantities of the plasmid, the antibiotic resistance of numerous bacteria is taken advantage of. Since numerous plasmids contain genes for antibiotic resistance naturally, it is possible to grow a bacterial cell culture in a media containing a specific antibiotic for which resistance genes are found in the plasmid. In this manner, only the bacteria that are transfected with the plasmid survive. Furthermore, microscopy can be coupled to other experimental techniques such as *microfluidics* devices [67] also referred to as a "lab on a chip" [121]. These are devices in which channels allows for the manipulation of small amounts of fluids, more precisely in the order of 10^{-8} to 10^{-9} litres [117], and at these scales the mixing of the various fluids in the system is minimal since it is limited by diffusion. This gives the researchers a high level of control over the environment in which single cells can be studied.

The study of individual yeast cells using microfluidics is enabled in three steps. Firstly, the device which is typically made of a polymer material such as thermoplastics [119] can be generated through 3D printing [114] where the design is based on fluid dynamics simulations. Secondly, the device is coupled to a systems of pumps which grants the researcher complete control of growth conditions such as availability of nutrients. Also, this type of experimental setup is also suitable for studying how single cells respond to sudden shifts in the availability and composition of nutrients in the environment [24]. Thirdly, using laser based techniques such as optical tweezers [119], it is possible to capture as well as move individual yeast cells and thereby generate high quality data of single cells. In summary, it is these techniques that enables the generation of experimental data that can be used to validate and calibrate mathematical models of protein kinetics. Thus, provided this knowledge of

the biological aspects of protein kinetics the proceeding section switches focus to the theoretical aspects of the topic at hand.

2.2 The construction, analysis and validation of mechanistic mathematical models of protein kinetics

The fundamental assumption of mechanistic modelling is that the cell is viewed as a chemical reactor. Accordingly, the cell is an enclosed volume where various reactions take place which in the context of this thesis corresponds to the formation and degradation of proteins. Mathematically, the description of the change in the quantity or concentration of proteins over time is described by systems of *ordinary differential equations (ODEs)*. In this chapter, we consider two (in certain cases one) proteins described by the functions $U, V : \mathbb{R}_+ \mapsto \mathbb{R}$ which satisfy the following system of ODEs

$$\begin{aligned} \frac{dU}{dt} &= F(U(t), V(t), \mathbf{k}) \\ \frac{dV}{dt} &= G(U(t), V(t), \mathbf{k}) \\ U(0) &= U_0 \text{ and } V(0) = V_0. \end{aligned} \tag{2.1}$$

The solutions, also referred to as the *states*, of (2.1) are the concentrations of the proteins $U(t)$ and $V(t)$ at time $t \in \mathbb{R}_+$. The reactions governing the dynamics are determined by the non-linear functions F and G which depend on the concentration of the proteins, the time and the kinetic rate parameters which are gathered in the vector $\mathbf{k} \in \mathbb{R}_+^p$ where $p \in \mathbb{N}_+$ is the number of parameters. Lastly, the initial concentration of the proteins, which mathematically are called the initial conditions, are given by the constants $U_0, V_0 \in \mathbb{R}_+$. Here, physically reasonable solutions corresponds to non-negative concentrations, i.e. $U(t), V(t) \geq 0 \forall t \in \mathbb{R}_+$. Another assumption underlying the ODE based model is that the concentrations of the proteins are *homogeneous* in the cell, which in certain cases is not plausible to assume.

In certain situations, the concentration of the proteins depend on both time and space. To account for this, let $\Omega \subset \mathbb{R}^n$ for $n = 1, 2$ or 3 denote the spatial domain which in this thesis is the interior of the cell, i.e. the cytosol, and $\Gamma \subset \mathbb{R}^{n-1}$ be its boundary which in this thesis is the cell membrane. Then, the

two proteins are described by the multivariate functions $U, V : \Omega \times \mathbb{R}_+ \mapsto \mathbb{R}$ which satisfy the following system of *partial differential equations* (PDEs)

$$\begin{aligned}
 \frac{\partial U}{\partial t} &= F(U(\mathbf{x}, t), V(\mathbf{x}, t), \mathbf{k}) + D_1 \Delta U, & \mathbf{x} \in \Omega, t \in \mathbb{R}_+ \\
 \frac{\partial V}{\partial t} &= G(U(\mathbf{x}, t), V(\mathbf{x}, t), \mathbf{k}) + D_2 \Delta V, & \mathbf{x} \in \Omega, t \in \mathbb{R}_+ \\
 U(\mathbf{x}, 0) &= U_0(\mathbf{x}) \ \& \ V(\mathbf{x}, 0) = V_0(\mathbf{x}), & \mathbf{x} \in \Omega \\
 D_1 \nabla U^T \mathbf{n} &= H_1(U(\mathbf{x}, t), V(\mathbf{x}, t)), & \mathbf{x} \in \Gamma, t \in \mathbb{R}_+ \\
 D_2 \nabla V^T \mathbf{n} &= H_2(U(\mathbf{x}, t), V(\mathbf{x}, t)), & \mathbf{x} \in \Gamma, t \in \mathbb{R}_+.
 \end{aligned} \tag{2.2}$$

This particular type of PDEs are called *reaction diffusion* (RD) equations. The solutions to the RD-system in (2.2) are the concentration of the proteins $U(\mathbf{x}, t)$ and $V(\mathbf{x}, t)$ at spatial coordinate $\mathbf{x} \in \Omega$ at time $t \in \mathbb{R}_+$. The meaning of the terms is similar to the ODE based model in (2.1) with the addition of the spatial dependence. The movement in space is determined by the process of diffusion which is mathematically described by the Laplace operator $\Delta = \sum_{i=1}^n \partial^2 / \partial x_i^2$ where x_i is the i^{th} spatial coordinate [59]. Here, the diffusion coefficients of the proteins U and V are given by D_1 and D_2 respectively. Also, there are boundary conditions determined by the functions H_1 and H_2 where $\nabla = (\partial / \partial x_1, \dots, \partial / \partial x_n)^T$ is the gradient, “ T ” is the transpose operator and $\mathbf{n} \in \mathbb{R}^n$ is the outward normal at $\mathbf{x} \in \Gamma$. Now, kinetic modelling entails the analysis of the solutions of (2.1) and (2.2) which hinges on the fact that such solutions actually exist.

If the reaction terms satisfy certain regularity conditions, there exist solutions to both the ODE and RD based models. If the reaction terms, e.g. F and G , are “nice”¹⁶ enough, there exist solutions to the system of ODEs in (2.1) which follows from the Picard-Lindelöf theorem [105] based on Banach’s fixed point theorem [18]. For the RD-model in (2.2), similar existence properties can be proven using fixed point arguments¹⁷ provided that the reaction terms are quasi-positive and take on a “mass control structure” [83]. Throughout this thesis, the reaction terms F and G are polynomial or at least continuous with continuous first derivatives, denoted \mathcal{C}^1 , which guarantees¹⁸ the existence of solutions to both the system of ODEs in (2.1) and the RD system in (2.2). Given this knowledge, let us now describe the general workflow implemented in mechanistic modelling.

¹⁶By “nice” we mean continuous and Lipschitz continuous.

¹⁷See the proof of Theorem 1 in Paper IV.

¹⁸At least for most open, bounded and regular domains $\Omega \in \mathbb{R}^n$ with smooth boundaries.

An overall aim of mechanistic modelling is to predict unknown biological properties using simulations. The first step in achieving this goal is to construct a model which is usually based on biological knowledge found in the literature. When a model is constructed, there are two approaches for analysing the model stemming from different research fields. The older of the two fields is mathematical biology which uses analytical methods such as linear stability analysis or symmetry methods to analyse the properties of the models which can be based on both ODEs (2.1) and PDEs (2.2). However, with the emergence of technologies enabling the gathering of large quantities of experimental data, a newer more empirical field called systems biology has emerged. Here, one common class of models consists of systems of ODEs, e.g. (2.1), and a large emphasis is on the validation of the models using experimental data where model parameters are calibrated by some measured experimental output. This validation is based on statistical methods which places the field of systems biology in between statistical and mechanistic modelling described in the introduction (Fig 1.1 on page 2). Although there is no clear distinction between the fields, it is rather the emphasis and tradition that differ slightly. An approximate workflow is presented below (Fig 2.2) and the disposition of the subsequent section is based on this workflow.

Initially, the construction of mechanistic models is described. Thereafter, the mathematical tool called linear stability analysis is presented followed by a description of the different numerical methods used to solve the ODE models in (2.1) and RD models in (2.2). Then, the validation of ODE models using experimental data is described including a description of the concepts parameter estimation, numerical identifiability and model selection. Thereafter, the mathematical tool of symmetry methods is presented within the context of mechanistic models. Lastly, based on a similar theoretical framework to the one used in the context of symmetries, a theoretical version of the notion of identifiability called structural identifiability is described.

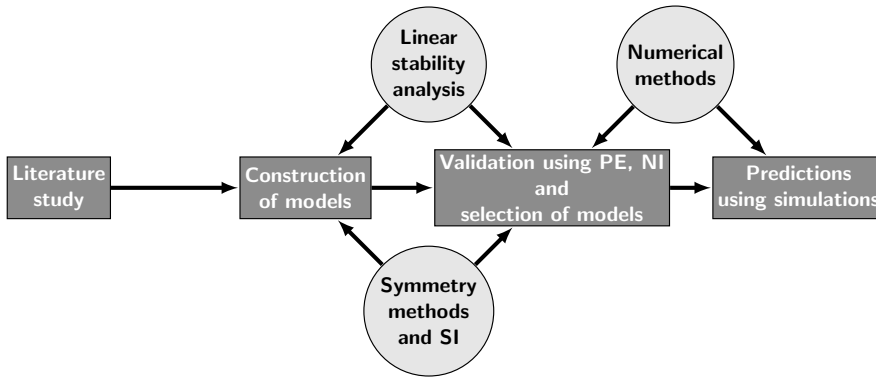


Figure 2.2: Workflow in mechanistic modelling within systems and mathematical biology. The workflow in systems biology illustrated by the squares consists of a literature study leading to the construction of a mechanistic model. The validation of this model using experimental data typically consists of *parameter estimation (PE)*, and *numerical identifiability (NI)* analysis. Lastly, the simulations of the validated model can be used to make predictions regarding unknown outcomes. In mathematical biology, illustrated by the circles, mathematical techniques such as linear stability analysis, symmetry methods and various numerical methods are implemented to analyse the properties of a model of interest. Using symmetry methods it is possible to analyse the mathematical properties of models based on differential equations and, using a similar approach, a theoretical version of the identifiability analysis called *structural identifiability (SI)* analysis can be conducted.

2.2.1 Construction of kinetic models and non-dimensionalisation

The construction of kinetic models is based on the *law of mass action*. This law states that the rate of a chemical reaction is proportional to the concentration of the involved species [58]. To exemplify its usage, let us consider the enzymatically catalysed conversion of a substrate S to a product P aided by the enzyme E where the intermediary substrate-enzyme complex is denoted C (Fig 2.3). The corresponding dynamics is governed by three reaction rates

$$r_1 = k_1 SE, \quad r_{-1} = k_{-1}C \quad \text{and} \quad r_2 = k_2 C$$

where all these terms have the units “concentration per time unit”. Now, if S , E , C and P have the unit concentration it implies that the kinetic rate constants k_{-1} and k_2 have the unit “per time” while the kinetic rate constant k_1 has the

unit “per concentration per time”. Moreover, by summing these reactions using the logic “formation subtracted by degradation” it is possible to describe the dynamics of this system mathematically.

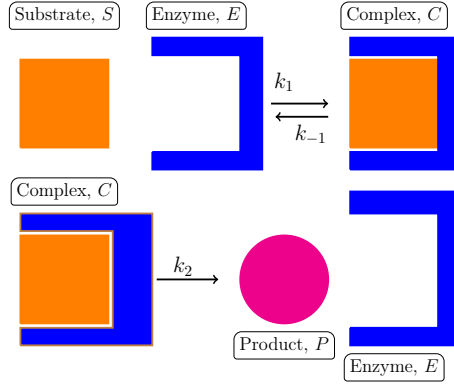


Figure 2.3: An enzymatically catalysed reaction. The substrate S is converted to the product P catalysed by the enzyme E by forming an intermediary complex C .

The mechanistic model of the enzymatically catalysed substrate-to-product conversion is given by the following system of ODEs (2.3)

$$\begin{aligned}
 \frac{dS}{dt} &= k_{-1}C - k_1SE \\
 \frac{dE}{dt} &= -\frac{dC}{dt} = (k_{-1} + k_2)C - k_1SE \\
 \frac{dP}{dt} &= k_2C
 \end{aligned} \tag{2.3}$$

$$S(0) = S_0, E(0) = E_{\text{tot}} \text{ and } C(0) = P(0) = 0.$$

Here, the initial conditions are S_0 for the substrate, E_{tot} for the enzyme and there are no complex molecules or products present initially. Further, under the assumption that $S_0 \gg E_{\text{tot}}$ it is possible to show¹⁹ that the dynamics of this system is governed by the classic Michaelis-Menten equation (2.4) [23, 58, 76]

¹⁹A generalised description of this enzymatically catalysed system, and some elaboration on the meaning of the involved assumptions as well as the involved parameters are found in Paper V.

$$\frac{dP}{dt} = -\frac{dS}{dt} = v_{\max} \frac{S}{K_M + S} \quad (2.4)$$

$$S(0) = S_0, \text{ and } P(0) = 0.$$

The involved parameters in the reduced version (2.4) are functions of the original kinetic rate parameters in (2.3), and even though they are not explained fully here the important point is the following. The law of mass action yields polynomial reaction functions, e.g. F and G in (2.1) and (2.2) respectively, and using simplifying assumptions it is possible to obtain polynomially bounded²⁰ non-linearities as in (2.4). Thus, using this type of methodology for constructing the kinetic models, solutions to both the ODE based models in (2.1) and the RD based models in (2.2) are guaranteed.

In addition, a common technique in mathematical biology is called non-dimensionalisation. This entails the scaling of the states and the variable in order to render them dimensionless [76]

$$u = \frac{1}{C_1}U, \quad v = \frac{1}{C_1}V \text{ and } \tau = \frac{1}{k}t$$

for some concentration C_1 and some first order kinetic rate parameter k . The advantage of the resulting model is that the parameters (which we will denote θ in the dimensionless case as oppose to \mathbf{k}) which themselves also are dimensionless are usually fewer in number and they are more meaningful compared to the original parameters as more properties are captured by them. Consequently, the original ODE model in (2.1) is re-written after it is non-dimensionalised in the following manner (2.5)

$$\begin{aligned} \frac{du}{d\tau} &= f(u(\tau), v(\tau), \theta) \\ \frac{dv}{d\tau} &= g(u(\tau), v(\tau), \theta) \\ u(0) &= u_0 \text{ and } v(0) = v_0. \end{aligned} \quad (2.5)$$

In a similar manner, the RD-models in (2.2) can be rendered dimensionless.

²⁰See [94] for how the Hill-equation is bounded mathematically.

Here, it is often the case that a particular non-dimensionalisation is implemented so as to give rise to the following exact structure of the models (2.6)

$$\begin{aligned}
 \frac{\partial u}{\partial \tau} &= \gamma f(u(\mathbf{x}, \tau), v(\mathbf{x}, \tau), \theta) + \Delta f, & \mathbf{x} \in \Omega, \tau \in \mathbb{R}_+ \\
 \frac{\partial v}{\partial \tau} &= \gamma g(u(\mathbf{x}, \tau), v(\mathbf{x}, \tau), \theta) + d\Delta g, & \mathbf{x} \in \Omega, \tau \in \mathbb{R}_+ \\
 u(\mathbf{x}, 0) &= u_0(\mathbf{x}) \text{ and } v(\mathbf{x}, 0) = v_0(\mathbf{x}), & \mathbf{x} \in \Omega \\
 \nabla u^T \mathbf{n} &= h_1(u(\mathbf{x}, \tau), v(\mathbf{x}, \tau)), & \mathbf{x} \in \Gamma, \tau \in \mathbb{R}_+ \\
 d\nabla v^T \mathbf{n} &= h_2(u(\mathbf{x}, \tau), v(\mathbf{x}, \tau)), & \mathbf{x} \in \Gamma, \tau \in \mathbb{R}_+.
 \end{aligned} \tag{2.6}$$

Here, the crucial parameters are the *relative reaction strength* γ and the *relative diffusion rate* d [75, 76]. By implementing a non-dimensionalisation giving rise to this exact structure, the relative magnitude of these parameters indicate if the dynamics of the system is dominated by the involved reactions or diffusion. Now that the technique for constructing models has been explained, mathematical tools for analysing the solutions to the models will be explained subsequently.

2.2.2 Solutions of linear systems of ODEs and linear stability

One of the few cases in which the exact solutions to a system of ODEs is known is in the case of a linear system. More precisely, assume that the reaction terms are of the form $f(u, v) = c_1 u + c_2 v$ and $g(u, v) = c_3 u + c_4 v$. Then, the system of ODEs in (2.5) can be written as follows (2.7)

$$\underbrace{\frac{d}{d\tau} \begin{pmatrix} u \\ v \end{pmatrix}}_{=\mathbf{u}} = \underbrace{\begin{pmatrix} c_1 & c_2 \\ c_3 & c_4 \end{pmatrix}}_{=A} \underbrace{\begin{pmatrix} u \\ v \end{pmatrix}}_{=\mathbf{u}} \Leftrightarrow \frac{d\mathbf{u}}{d\tau} = A\mathbf{u}. \tag{2.7}$$

Moreover, assume that the matrix $A \in \mathbb{R}^{2 \times 2}$ is *diagonalisable*, i.e. that there exists two matrices $D, P \in \mathbb{C}^{2 \times 2}$ of the following type

$$D = \begin{pmatrix} \lambda_1 & 0 \\ 0 & \lambda_2 \end{pmatrix} \text{ \& } P = (\mathbf{v}_1 \quad \mathbf{v}_2)$$

where $\lambda_1, \lambda_2 \in \mathbb{C}$ are the eigenvalues of A and $\mathbf{v}_1, \mathbf{v}_2 \in \mathbb{C}^2$ are the correspond-

ing eigenvectors²¹ so that $AP = PD \Leftrightarrow D = P^{-1}AP$. Then, the coordinate change²² given by $\mathbf{y} = P^{-1}\mathbf{u} \Leftrightarrow \mathbf{u} = P\mathbf{y}$ yields the following calculations

$$\begin{aligned} \frac{d\mathbf{y}}{d\tau} &= P^{-1} \frac{d\mathbf{u}}{d\tau} = P^{-1}A\mathbf{u} \\ &= P^{-1}AP\mathbf{y} = D\mathbf{y} \\ \implies \dot{\mathbf{y}} &= D \cdot \mathbf{y} \\ \Leftrightarrow \frac{d}{d\tau} \begin{pmatrix} y_1(\tau) \\ y_2(\tau) \end{pmatrix} &= \begin{pmatrix} \lambda_1 & 0 \\ 0 & \lambda_2 \end{pmatrix} \begin{pmatrix} y_1(\tau) \\ y_2(\tau) \end{pmatrix} = \begin{pmatrix} \lambda y_1(\tau) \\ \lambda_2 y_2(\tau) \end{pmatrix} \end{aligned}$$

which results in two separable ODEs with respect to the states in \mathbf{y} . The corresponding solutions are given by $y_1(\tau) = C_1 e^{\lambda_1 \tau}$ and $y_2(\tau) = C_2 e^{\lambda_2 \tau}$ for some arbitrary constants $C_1, C_2 \in \mathbb{R}$. Lastly, by transforming back to the original states using $\mathbf{u} = P\mathbf{y}$, it is possible to show that the solutions of (2.7) is given by a linear combination of the eigenvectors

$$\mathbf{u}(\tau) = C_1 \mathbf{v}_1 e^{\lambda_1 \tau} + C_2 \mathbf{v}_2 e^{\lambda_2 \tau}. \quad (2.8)$$

Next, we define the concept of a *steady state* which will subsequently allow us to define the concept of linear stability. A steady state $\mathbf{u}^* = (u^* \ v^*)^T \in \mathbb{R}_+^2$ is a vector satisfying

$$\frac{d\mathbf{u}^*}{d\tau} = \mathbf{0}$$

and since A is diagonalisable it is also invertible. This implies that there exist only one steady-state to (2.7) namely the trivial vector $\mathbf{u}^* = \mathbf{0}$. Now, the concept of linear stability means that the trajectories of the solutions to (2.7) converge to the steady state after a long time, i.e. $\lim_{\tau \rightarrow \infty} \mathbf{u}(\tau) = \mathbf{u}^* = \mathbf{0}$. By the explicit formula for the solutions in (2.8), this implies that the original system in (2.7) is stable (in the sense of linear stability) if and only if the real parts of the eigenvalues are negative, i.e. $\text{Re}(\lambda_1), \text{Re}(\lambda_2) < 0$. In addition, it can be shown that the eigenvalues²³ of the matrix A in (2.7) are given by

²¹An eigenvector $\mathbf{v} \in \mathbb{C}^2$ to a matrix $A \in \mathbb{R}^2$ is a non-trivial vector such that $A\mathbf{v} = \lambda\mathbf{v}$ where the scalar $\lambda \in \mathbb{C}$ is called the eigenvalue of A

²²This change of coordinates is well-known, but can be found in [42].

²³The eigenvalues are, in general, given by solving the *characteristic equation* $\det(A - \lambda I) = 0$

$$\lambda_{1,2} = \frac{1}{2} \left(\text{Tr}(A) \pm \sqrt{\text{Tr}(A)^2 - 4 \det(A)} \right) \quad (2.9)$$

where $\text{Tr}(A) = c_1 + c_4$ is the *trace* and $\det(A) = c_1c_4 - c_2c_3$ is the *determinant* of the matrix A . This implies that the system (2.7) is *stable*, or that the steady state $\mathbf{u}^* = \mathbf{0}$ is a *stable node*, if the conditions $\text{Tr}(A) < 0$ and $\det(A) > 0$ hold. Other common types of dynamics are an *unstable node* corresponding to $\text{Tr}(A) > 0$ and $\det(A) > 0$ and a *saddle point* corresponding to $\det(A) < 0$ [23].

Although most of the systems encountered in kinetic modelling are not linear, the same type of mathematics can be implemented for analysing the stability of non-linear systems.

2.2.3 Linear stability analysis of non-linear systems

A linear stability analysis of a non-linear system (2.5) or (2.6) is *local* with respect to the steady-states. In the case of the non-linear systems, a steady-state $\mathbf{u}^* = (u^* \ v^*)^T \in \mathbb{R}_+^2$ is a solution to the equations given by $f(u^*, v^*) = g(u^*, v^*) = 0$. Furthermore, the first order Taylor expansion of these functions around the steady states are given by

$$\begin{aligned} f(u, v) &= \underbrace{f(u^*, v^*)}_{=0} + \left. \frac{\partial f}{\partial u} \right|_{(u,v)=(u^*,v^*)} \cdot (u - u^*) + \left. \frac{\partial f}{\partial v} \right|_{(u,v)=(u^*,v^*)} \cdot (v - v^*) \\ &\quad + \mathcal{O} \left(\begin{pmatrix} u - u^* \\ v - v^* \end{pmatrix}^2 \right) \\ \Leftrightarrow f(u, v) &= \left(\nabla f|_{(u,v)=(u^*,v^*)} \right)^T \cdot \begin{pmatrix} u - u^* \\ v - v^* \end{pmatrix} + \mathcal{O} \left(\begin{pmatrix} u - u^* \\ v - v^* \end{pmatrix}^2 \right) \end{aligned}$$

where $I \in \mathbb{R}^{2 \times 2}$ is the identity matrix. In the particular case of a two dimensional system, the characteristic polynomial is a second order polynomial with the corresponding solutions given by (2.9).

and

$$g(u, v) = \underbrace{g(u^*, v^*)}_{=0} + \left. \frac{\partial g}{\partial u} \right|_{(u,v)=(u^*,v^*)} \cdot (u - u^*) + \left. \frac{\partial g}{\partial v} \right|_{(u,v)=(u^*,v^*)} \cdot (v - v^*) + \mathcal{O} \left(\begin{pmatrix} u - u^* \\ v - v^* \end{pmatrix}^2 \right)$$

$$\Leftrightarrow g(u, v) = \left(\nabla g|_{(u,v)=(u^*,v^*)} \right)^T \cdot \begin{pmatrix} u - u^* \\ v - v^* \end{pmatrix} + \mathcal{O} \left(\begin{pmatrix} u - u^* \\ v - v^* \end{pmatrix}^2 \right).$$

Now, let us introduce the following *local coordinate*

$$\mathbf{w} = \begin{pmatrix} u - u^* \\ v - v^* \end{pmatrix}.$$

Then, a simple calculation allows us to rewrite the time derivatives

$$\frac{du}{d\tau} = \frac{du}{d\tau} - \underbrace{\frac{du^*}{d\tau}}_{=0} = \frac{d(u - u^*)}{d\tau} \text{ and similarly } \frac{dv}{d\tau} = \frac{d(v - v^*)}{d\tau}$$

which shows that $du/d\tau = dw/d\tau$. All of these expressions can be summarised by equation (2.10) which is the linearisation²⁴ of (2.5) around a steady state.

$$\frac{d}{d\tau} \underbrace{\begin{pmatrix} u - u^* \\ v - v^* \end{pmatrix}}_{=\mathbf{w}} = \underbrace{\begin{pmatrix} \left. \frac{\partial f}{\partial u} \right|_{(u,v)=(u^*,v^*)} & \left. \frac{\partial f}{\partial v} \right|_{(u,v)=(u^*,v^*)} \\ \left. \frac{\partial g}{\partial u} \right|_{(u,v)=(u^*,v^*)} & \left. \frac{\partial g}{\partial v} \right|_{(u,v)=(u^*,v^*)} \end{pmatrix}}_{=J(u^*,v^*)} \underbrace{\begin{pmatrix} u - u^* \\ v - v^* \end{pmatrix}}_{=\mathbf{w}} \quad (2.10)$$

$$\Leftrightarrow \frac{d\mathbf{w}}{d\tau} = J(u^*, v^*) \mathbf{w}$$

Here, the matrix J is called the Jacobian matrix and the concept of linear stability applies locally to non-linear systems in proximity of the steady states.

²⁴By linearisation we mean the truncated (i.e. higher order terms are omitted) first order Taylor expansion.

Thus, we can summarise how a linear stability analysis of a non-linear system of ODEs as in (2.5) is conducted in a three part recipe:

1. Calculate the steady states (u^*, v^*) of the system by solving the equations, $f(u^*, v^*) = g(u^*, v^*) = 0$,
2. Derive the Jacobian matrix $J(u, v)$ in (2.10) as a function of the states u and v ,
3. Plug in each steady state into the Jacobian matrix, and analyse the stability properties of the resulting matrices $J(u^*, v^*)$.

Specifically with regards to the spatial RD models in (2.6) on page 22, there is a particularly interesting phenomena called *diffusion-driven instability* [75]. This corresponds to the fact that the homogeneous²⁵ system of (2.6) with the following linearisation

$$\frac{d\mathbf{w}}{d\tau} = \gamma J(u^*, v^*)\mathbf{w}$$

is stable. This implies that (u^*, v^*) is a stable node and here the parameter γ , which is common in numerous dimensionless RD-models, is the strength of the reaction term. Furthermore, the linearisation of the inhomogeneous system in (2.6) given by

$$\frac{d\mathbf{w}}{d\tau} = \gamma J(u^*, v^*)\mathbf{w} - k^2 D\mathbf{w} \quad \text{where} \quad D = \begin{pmatrix} 1 & 0 \\ 0 & d \end{pmatrix}$$

is unstable implying that (u^*, v^*) is an unstable node for the latter system where k^2 is the *wave number*²⁶. In other words, the introduction of diffusion changes the stability of the system from a stable to an unstable node and hence the name *diffusion-driven instability*. This phenomena was originally proposed by Alan Turing [108] in order to model morphogenesis but it is also used to model for example pattern formation in the context of animal coatings [75].

A linear stability analysis allows modellers to predict the long term behaviour of a dynamic system in terms of the involved kinetic parameters. However, to find the solution of a model in order to generate particular simulations of a given system it is common to resort to numerical methods.

²⁵By the homogeneous system of (2.6), we mean the ODE-system neglecting the terms corresponding to diffusion.

²⁶The wave numbers are the eigenvalues of the Laplace operator Δ .

2.2.4 Numerical methods for solving differential equations

There are two major methodologies for solving differential equations, namely *finite differences (FD)* and the *finite element method (FEM)*. In the context of this thesis, FD based methodologies are used to solve the ODE based model in (2.5) and to discretise the time derivatives in the RD models in (2.6). Moreover, in this thesis the FEM is used to discretise the spatial aspects of the RD models in (2.6).

The FD based methodologies are based on approximating derivatives with differences. To exemplify this approach, consider the first order ODE

$$\frac{du}{d\tau} = f(u(\tau)), \quad u(0) = u_0$$

with reaction term f and initial condition u_0 . Then, the first step of all FD based numerical schemes is to discretise the time line into discrete nodes. For example, a discretisation of the interval $[0, T]$ for some end time $T \in \mathbb{R}_+$ with $n \in \mathbb{N}_+$ nodes is $\mathcal{T}_k := \{t_i = i \cdot k, \text{ with } i = 0, 1, \dots, n + 1 \text{ and } k = T/n\}$ where a homogeneous step size k is implemented. After this, the time derivatives are approximated by finite differences as follows

$$\left. \frac{du}{d\tau} \right|_{t=t_i} \approx \frac{u(t_i) - u(t_{i-1})}{k}.$$

The different solution algorithms associated with these methods calculate the concentration $u(t_i)$ at the current time node t_i from the known previous concentrations $u(t_{i-1})$ at the previous time node t_{i-1} . In this way, FD algorithms entail the construction of a *time-stepping scheme* in which the numerical scheme “jumps forward” along the nodes in \mathcal{T}_k . Moreover, what classifies a FD based method is how the reaction term in the right hand side is approximated. The two major approaches are the *explicit*²⁷ or the *implicit*²⁸ FD method.

$$\frac{u(t_i) - u(t_{i-1})}{k} = \begin{cases} f(u(t_{i-1})), & \text{Explicit} \\ f(u(t_i)), & \text{Implicit} \end{cases}$$

The former method is cheaper and thereby faster to compute than the latter as the non-linear reaction function is evaluated at the “known” previous time

²⁷Also called the forward Euler method.

²⁸Also called the backward Euler method.

node. However, the explicit method has worse stability properties than the implicit approach as it is merely conditionally stable for small values of k while the implicit approach is unconditionally stable [13, 46]. In addition, for certain problems with a particular dynamics it is beneficial from a performance perspective to use a non-homogeneous step size k in the discretisation \mathcal{T}_k .

For so called stiff problems, it is advantageous to use an adaptive step size. Such an ODE is stable where the dynamics is dominated by one of the eigenvalues which is large and negative implying that the system will reach a steady-state. A consequence of this is that the dynamics is characterised by a quick change in concentrations initially while the change is very small for larger times close to when the steady state is reached. For this type of problems, which are very common in mechanistic modelling in mathematical and systems biology, it is computationally beneficial to use a small time step k for small times while it the step size can be increased for larger times without losing computational accuracy. An adaptive step size, which numerous algorithms specialised for solving stiff problems use, is based on an approximation of the *residual* which is a measure of how the big the error between the actual solution and the current approximation is. Given this setting, these types of algorithms increase the step size k when the residual is small and decreases the step size when the residual is large. Examples of adaptive methods are the various *Runge-Kutta* (RK) methods [13, 46] where the RK45 method, for example, uses a fourth and fifth order Taylor approximation in order to estimate the residual which is used as a basis for choosing the adaptive step size. For spatial problems such as the RD models in (2.6), it is common to implement a FEM to discretise the spatial aspects of the model.

The FEM is based on distribution theory within functional analysis [18, 43, 59]. To illustrate its implementation, consider the one-species RD-model in (2.6) (i.e. $g = h_2 = v_0 = 0$) with Neumann boundary conditions, i.e. $h_1 = 0$. Then, we multiply the PDE with a *test function* $\phi \in \mathcal{C}_0^1(\Omega)$ and integrate over the domain

$$\langle \partial_t u, \phi \rangle = \gamma \langle f(u), \phi \rangle + \langle \Delta u, \phi \rangle \quad (2.11)$$

where “ $\langle \cdot, \cdot \rangle$ ”²⁹ means the \mathcal{L}^2 -inner product defined by

$$\langle f, g \rangle = \int_{\Omega} f(\mathbf{x})g(\mathbf{x}) \, d\mathbf{x} \implies \langle f, f \rangle = \|f\|^2$$

²⁹The proper notation would be “ $\langle \cdot, \cdot \rangle_{\mathcal{L}^2(\Omega)}$ ”.

for two functions f, g such that the integral over Ω is defined³⁰. Here, as is the case with all inner products, a norm denoted “ $\|\cdot\|$ ”³¹ is induced. Further, in similarity to integration by parts, it is possible to define the *weak derivative* of a $\mathcal{L}^2(\Omega)$ -function v by

$$D^\alpha v(\phi) = (-1)^{|\alpha|} \int_{\Omega} v D^\alpha \phi dx \quad \text{for} \quad \begin{cases} D^\alpha \phi &= \frac{\partial^{|\alpha|} \phi}{\partial x_1^{\alpha_1} \partial x_2^{\alpha_2} \dots \partial x_n^{\alpha_n}} \\ \alpha &= (\alpha_1 \quad \alpha_2 \quad \dots \quad \alpha_n), \quad |\alpha| = \sum_{i=1}^n \alpha_i \end{cases}$$

which means that the (spatial) derivatives fall on the “nice” (i.e. infinitely differentiable) test function. Then, we can define a *Sobolov space* [59, 18] as follows

$$\mathcal{H}^k(\Omega) := \{v \in \mathcal{L}^2(\Omega) : D^\alpha v \in \mathcal{L}^2(\Omega) \text{ for } |\alpha| \leq k\}$$

for any $k \geq 1$ and it is in this type of function spaces that the solution u should lie. Note here that it is not assumed that the solution u is differentiable in the sense of regular functions but rather in terms of weak derivatives, and functionals defined by the integral of an integrand composed of a test function are the subject of distribution theory³². Nevertheless, for the purpose of illustrating the methodology, we think of the solution as a regular function, i.e $u \in \mathcal{C}^2(\Omega)$.

Next, we rewrite the diffusive term in (2.11) using Green’s identity [59] which in the case of Neumann boundary conditions becomes $\langle \Delta u, \phi \rangle = -\langle \nabla u, \nabla \phi \rangle$. This yields the classical *variational formulation (VF)* which is a reformulation of the original problem

$$\text{Find } u \in H^1(\Omega) \text{ such that} \tag{2.12}$$

$$\langle \partial_\tau u, \phi \rangle + \langle \nabla u, \nabla \phi \rangle - \gamma \langle f(u), \phi \rangle = 0 \quad \forall \phi \in H^1(\Omega).$$

Note here that if $u \in \mathcal{C}^2(\Omega)$ and satisfies (2.12) it is exactly the classical solution to the original problem. However, the number of objects³³ u that solves (2.12) is larger than the functions $u \in \mathcal{C}^2(\Omega)$ solving the original problem, and this

³⁰In fact, this type of integral defines the well-known $\mathcal{L}^2(\Omega)$ -vector space defined as

$$\mathcal{L}^2(\Omega) := \left\{ \text{Functions } f(\mathbf{x}), \mathbf{x} \in \Omega : \|f\|_{\mathcal{L}^2(\Omega)}^2 = \langle f, f \rangle_{\mathcal{L}^2(\Omega)} < \infty \right\}.$$

³¹The proper notation would be “ $\|\cdot\|_{\mathcal{L}^2(\Omega)}$ ”.

³²For further reading, see [18, 43].

³³Specifically, these objects are distributions.

mathematical framework captured by distribution theory expands the notion of differential equations to a larger set of, for example, discontinuous objects which often occur in applications³⁴.

The method proceeds by discretising the spatial domain implying the generation of a *mesh*. Then, a space of discrete test functions V_h is employed and this space typically consists of piecewise continuous linear functions on the mesh and it is in this space³⁵ that the approximation lies. More precisely, the approximate solution based on the FEM to the original problem is the projection, in the sense of the \mathcal{L}^2 -inner product, of the VF onto the discrete space V_h .

Now, that the methodology for simulating kinetic models is presented, these simulations can be used in order to calibrate a model using experimental data.

2.2.5 Model validation, estimation of kinetic parameters (PE), numerical identifiability (NI) and selection of models

Assume that an ODE based model as in (2.5) is to be validated using experimental data in the form of a time series³⁶. More precisely, assume that the observed output in the time series is theoretically described by the function \hat{y} and thus adding this to the model yields the following equation

$$\begin{aligned}\frac{du}{d\tau} &= f(u(\tau), v(\tau), \theta) \\ \frac{dv}{d\tau} &= g(u(\tau), v(\tau), \theta) \\ \hat{y}(\tau, \theta) &= o(u(\tau), v(\tau), \theta) \\ u(0) &= u_0 \text{ and } v(0) = v_0\end{aligned}\tag{2.13}$$

where the *simulated output* \hat{y} is determined by some³⁷ function o of the two states. Moreover, using the standard statistical approach based on a maximum likelihood derivation, the validation of the model entails finding the kinetic rate parameters $\theta \in \mathbb{R}_+^p$, $p \in \mathbb{N}_+$ giving rise to the simulations that best describe the measured data. Accordingly, the concept of validating a model implies

³⁴Two such examples are the Heaviside function and the Dirac delta, see [18]. The former is common in control theory when modelling an input of a system.

³⁵Sometimes the approximate solution lies in a slightly different space called the *trial space*.

³⁶For an idea of the experimental techniques used for generating the time series, see subsection 2.1.4 on page 14.

³⁷This function could for example be the quotient of the two states, i.e. $o(u(\tau), v(\tau)) = u(\tau)/v(\tau)$.

estimating the kinetic parameters which means that the validation of models and *parameter estimation (PE)* are closely connected.

To this end, assume that some output $y_i = y(\tau_i)$ has been measured at $N + 1$ time points denoted τ_i where $i \in \{0, \dots, N\}$ (Tab 2.1).

Table 2.1: Example of experimental data in the form of a time series.

Time, τ	Output, $y(\tau)$
$t_0 = 0$	$y_0 = 8$
$t_1 = 5$	$y_1 = 22$
$t_2 = 15$	$y_2 = 31$
$t_3 = 25$	$y_3 = 36$
\vdots	\vdots
$t_N = \dots$	$y_N = \dots$

Here, the corresponding simulated output with the given parameters are denoted $\hat{y}_i(\theta) = \hat{y}(\tau_i, \theta)$. Given this notation, we assume that the model corresponds to the true underlying process where the *error* between the simulated and measured output is normally distributed with zero mean and variance σ_i (2.14)

$$\left. \begin{aligned} e_i(\theta) &= y_i - \hat{y}_i(\theta) \\ e_i(\theta) &\sim \mathcal{N}(0, \sigma_i) \end{aligned} \right\}, \text{ for } i \in \{0, \dots, N\}. \quad (2.14)$$

Now, given the normality assumption (2.14), the following density function describes the probability of the model describing the data point (τ_i, y_i) [90]

$$p(e_i(\theta)) = \frac{1}{\sqrt{2\pi\sigma_i^2}} \exp\left(-\frac{e_i(\theta)^2}{2\sigma_i^2}\right).$$

Furthermore, assuming that the measurements are *independent and identically distributed (IID)* the joint probability distribution is given by the products of these densities [90]

$$P = \prod_{i=0}^N p(e_i(\theta)) = \prod_{i=0}^N \frac{1}{\sqrt{2\pi\sigma_i^2}} \exp\left(-\frac{e_i(\theta)^2}{2\sigma_i^2}\right).$$

Substituting the expression in (2.14) for the errors e_i in terms of the measured

and simulated output (i.e. y_i and \hat{y}_i respectively) yields

$$P(\theta) = \prod_{i=0}^N \frac{1}{\sqrt{2\pi\sigma_i^2}} \exp\left(-\frac{(y_i - \hat{y}_i(\theta))^2}{2\sigma_i^2}\right)$$

and by defining the *loglikelihood* as

$$L(\theta) = -\ln(P(\theta))$$

it is given by the following expression

$$L(\theta, \tilde{\sigma}) = \frac{1}{2} \sum_{i=0}^N \ln(2\pi\sigma_i^2) + \sum_{i=0}^N \left(\frac{(y_i - \hat{y}_i(\theta))^2}{2\sigma_i^2} \right) \quad (2.15)$$

$$\text{where } \vec{\sigma} = (\sigma_0 \quad \sigma_1 \quad \dots \quad \sigma_N)^T.$$

Now, the parameters are obtained using a maximum likelihood approach which can be formulated as follows

$$\text{Find } (\theta, \tilde{\sigma}) = \operatorname{argmin} L(\theta, \tilde{\sigma}). \quad (2.16)$$

In the case of constant variance, i.e.

$$\sigma_i = \sigma \quad \forall i \in \{0, \dots, N\}$$

the maximum likelihood approach (2.16) reduces to the classical *least square* problem

$$\text{Find } \theta = \operatorname{argmin} \text{LS}(\theta) := \operatorname{argmin} \sum_{i=0}^N (y_i - \hat{y}_i(\theta))^2. \quad (2.17)$$

In other words, the estimation of parameters implies selecting the kinetic parameters that minimise the Euclidian distance between the measured data and the simulated output in (2.16) and (2.17). In order to solve these optimisation

problems, the numerical methods described in the previous section in order to simulate the output \hat{y}_i must be implemented in combination with an optimisation algorithm. Commonly, a local continuous algorithm is used and closely connected to this type of algorithm is the concept of *numerical identifiability* (NI). To describe this more concretely, consider the least square problem in (2.17) and given this situation the algorithm proceeds as follows [3].

Algorithm 1: A continuous local optimisation algorithm in the context of PE

Output: The optimal parameter θ solving (2.17);

Input: An initial guess of the parameters, i.e. $\theta \leftarrow \theta_0 \in \mathbb{R}_+^p$;

- 1 **while** *Termination criteria is not satisfied* **do**
 - 2 *Descent direction:* Find a descent direction $\mathbf{p} \in \mathbb{R}_+^p$;
 - 3 *Line search:* Calculate a step length α such that $\text{LS}(\theta + \alpha\mathbf{p}) < \text{LS}(\theta)$;
 - 4 *Update:* Set $\theta \leftarrow \theta + \alpha\mathbf{p}$;
 - 5 **end**
-

The crucial step in Algorithm 1 is to compute a so called *descent direction* on line 2. Consider the linearisation of $\text{LS}(\theta)$ around the point “ $\theta + \mathbf{p}$ ”

$$\text{LS}(\theta + \mathbf{p}) = \text{LS}(\theta) + \nabla\text{LS}|_{\theta}^T \mathbf{p} \implies \boxed{\text{LS}(\theta + \mathbf{p}) - \text{LS}(\theta) = \nabla\text{LS}|_{\theta}^T \mathbf{p}}.$$

Now, since a minimisation problem is solved it is desirable to have a negative left hand side, i.e. $\text{LS}(\theta + \mathbf{p}) - \text{LS}(\theta) < 0 \implies \text{LS}(\theta + \mathbf{p}) < \text{LS}(\theta)$, implying that the cost function decreases in each step of the algorithm. Accordingly, a *descent direction* is defined as a vector $\mathbf{p} \in \mathbb{R}_+^p$ satisfying $\nabla\text{LS}|_{\theta}^T \mathbf{p} < 0$. The so called *steepest descent* algorithm chooses the descent direction according to the assignment “ $\mathbf{p} \leftarrow \left(-\nabla\text{LS}|_{\theta}^T\right)$ ” [3]. The advantage of this algorithm is that the descent direction is cheap to compute, but the drawback is that the overall algorithm converges slowly to the minima. An alternative algorithm which is computationally expensive but converges faster to the minima is the so called *Newton-Raphson* algorithm [3]. This algorithm uses the second order Taylor expansion

$$\text{LS}(\theta + \mathbf{p}) = \text{LS}(\theta) + \nabla\text{LS}|_{\theta}^T \mathbf{p} + \frac{1}{2}\mathbf{p}^T H(\theta)\mathbf{p}$$

where $H(\theta)$ is the so called Hessian matrix where its elements are the second

order partial derivatives, e.g.

$$H_{i,j}(\theta) = \frac{\partial^2}{\partial c_i \partial c_j} \text{LS}(\theta) \quad \text{for } i, j \in \{0, \dots, p\}$$

where the rate parameters are denoted $\theta = (c_1 \ c_2 \ \dots \ c_p)^T$. As was previously stated, this algorithm converges faster than the steepest descent counterpart due to the fact that it takes the curvature of the parameter space into account. The corresponding descent direction³⁸ in the case of the Newton-Raphson algorithm is given by solving

$$H(\theta)\mathbf{p} = -\nabla \text{LS}|_{\theta} \implies \boxed{\mathbf{p} \leftarrow H^{-1}(\theta) (-\nabla \text{LS}|_{\theta})}$$

However, the Hessian matrix is typically computationally expensive, so therefore it is common to use a so called *quasi Newton-Raphson* method which approximates the Hessian matrix using first order derivatives. In this way, the descent direction step of the algorithm is much faster than the original Newton-Raphson method but, simultaneously, it converges faster to the minima compared to the steepest descent algorithm. The approximation of the Hessian matrix is based on the so called *sensitivity matrix* S [19]

$$S = \begin{pmatrix} \left. \frac{\partial \hat{y}}{\partial c_1} \right|_{t=t_0} & \left. \frac{\partial \hat{y}}{\partial c_2} \right|_{t=t_0} & \cdots & \left. \frac{\partial \hat{y}}{\partial c_p} \right|_{t=t_0} \\ \left. \frac{\partial \hat{y}}{\partial c_1} \right|_{t=t_1} & \left. \frac{\partial \hat{y}}{\partial c_2} \right|_{t=t_1} & \cdots & \left. \frac{\partial \hat{y}}{\partial c_p} \right|_{t=t_1} \\ \vdots & \vdots & \ddots & \vdots \\ \left. \frac{\partial \hat{y}}{\partial c_1} \right|_{t=t_N} & \left. \frac{\partial \hat{y}}{\partial c_2} \right|_{t=t_N} & \cdots & \left. \frac{\partial \hat{y}}{\partial c_p} \right|_{t=t_N} \end{pmatrix} \quad (2.18)$$

which consists of the so called sensitivities “ $\partial \hat{y} / \partial c_i$ ” for $i \in \{1, \dots, p\}$ which correspond to the change in the output with respect to a specific parameter c_i . Using this matrix, the Hessian is approximated by the matrix $\boxed{\tilde{H} = S^T W S}$ where $W \in \mathbb{R}^{(N+1) \times (N+1)}$ is a weight matrix³⁹ corresponding to the variance in the data [19]. Also, the so called *covariance matrix* C can be approximated⁴⁰ using the sensitivity matrix S [19] according to

³⁸This is only true if the Hessian matrix is *positive definite*, that is if $\mathbf{p}^T H(\theta) \mathbf{p} > 0 \forall \mathbf{p} \in \mathbb{R}_+^p$.

³⁹In certain cases, the weight matrix is set to “ $W = (1/s^2)I$ ” where “ $s^2 = (1/N) \sum_{i=0}^N (y_i - \bar{y})^2$ ” is the overall variance in the data and $I \in \mathbb{R}^{(N+1) \times (N+1)}$ is the identity matrix [19].

⁴⁰This follows from the fact that \tilde{H} approximates the *Fisher information matrix (FIM)* and FIM is related to the covariance matrix C by the Cramer-Rao Inequality [19].

$$C = \text{cov}(\tilde{H}) = \tilde{H}^{-1}$$

and this enables us to define the notion of NI. Since the diagonal elements of the covariance matrix, denoted C_{ii} , corresponds to the variance of the i^{th} parameter one can study the *coefficient of variation* [19]

$$\sigma_{c_i} = \frac{\sqrt{C_{ii}}}{c_i}$$

where the variance of the parameter is scaled by the value of the parameter itself. It is also possible to calculate the *correlation matrix* from the covariance matrix C , and using this matrix in combination with the coefficient of variation σ_{c_i} it is possible to define NI. More precisely, a parameter c_i is said to be numerically identifiable if it has a low coefficient of variation, i.e. a low value of σ_{c_i} , and if it has low correlations with the other parameters. Another, more intuitive, way to think about identifiability is in terms of the sensitivities. Since the covariance matrix is calculated by taking the inverse of the Hessian matrix and since the Hessian matrix is directly approximated by the sensitivity matrix it follows that small values of the sensitivities result in a large coefficient of variation. In other words, if a parameter does not change the observed output, i.e. " $\partial \hat{y} / \partial c_i \approx 0$ " for $i \in \{1, \dots, p\}$ then the parameter will not be (numerically) identifiable.

Thus, the concept of model validation is closely connected to the terms PE and NI. In other words, two closely related questions that are often of interest when validating a model are "which parameters describe the data well?" (PE) and "given the observed data, which parameter can we actually estimate with precision?" (NI). Additionally, model validation combines three major fields of applied mathematics, namely statistics, optimisation and differential equations. A slightly different notion than the validation of models is that of *model selection* which is important if multiple candidate models are available. In this case, it is not only how well the models fit the data that is used as a basis for model selection but also the complexity of the models at hand.

Model selection can be done using two very well known information criteria. These are the Akaike Information Criteria (AIC) [6, 11, 31, 54, 103] and the corresponding information criteria based on Bayesian model selection called BIC [11, 31, 44, 54, 62, 103]. These can be formulated as follows [11]

$$\text{AIC} = L(\theta, \vec{\sigma}) + \tilde{\sigma}^2 \frac{2p}{N+1} \quad \text{and} \quad \text{BIC} = L(\theta, \vec{\sigma}) + p \frac{\ln(N+1)}{N+1} \quad (2.19)$$

where $\tilde{\sigma}^2$ is the variance of the experimental noise and p is the number of parameters. In the case of multiple time series, denote the number of time series by m , then the variance $\tilde{\sigma}^2$ is calculated using a classic estimator of the variance, namely $\tilde{s}^2 = (\sum_{i=1}^m (y - \bar{y})^2) / (m - 1)$. The model with the lowest selection criterias, i.e. the lowest values of AIC and BIC respectively, is chosen. Thus, it is not only a good fit implying a low value of $L(\theta, \tilde{\sigma})$ that is selected, but also a small model in terms of the number of parameters p . Consequently, the simplest model structure that best describes the data is selected using the statistical approach of model selection.

Besides this very data-driven way of describing the notion of identifiability, it is also possible to define this notion from a purely theoretical standpoint. Nevertheless, to be able to do this, mathematical concepts from differential geometry and group theory that are rarely used in data-driven sciences, such as systems biology, must be introduced. To this end, we will proceed by describing a theoretical tool for analysing differential equations, namely so called *symmetry methods* (subsection 2.2.6), which will subsequently enable us to mathematically analyse the identifiability of a given model (subsection 2.2.7).

2.2.6 Symmetry methods for differential equations

Symmetry methods use a geometrical approach⁴¹ to analyse differential equations. This way of thinking about these types of equations is quite unfamiliar for numerous researchers within mathematical and systems biology. Therefore, let us introduce the topic with an example.

Classically, when differential equations are studied, we tend to think about them from the perspective of analysis. In other words, we are interested in the functions that solve a particular differential equation and in this subsection we restrict ourselves to ODEs. Moreover, when studying models consisting of differential equations, it is of interest to find the solutions analytically through, for example, integrating factors or various transforms, or the focus is on determining the long term asymptotic behaviour of the solutions using linear stability analysis. As an example, consider the following ODE

$$\frac{du}{d\tau} = \frac{u}{\tau} \quad (2.20)$$

where the solution is the function $u(\tau)$ and τ is the variable. Now, the solution

⁴¹More precisely, it uses mathematics stemming from group theory, representation theory, and differential geometry.

to (2.20) is quite straightforward to calculate as the ODE is separable

$$\frac{du}{d\tau} = \frac{u}{\tau} \implies \frac{du}{u} = \frac{d\tau}{\tau} \implies \int \frac{du}{u} = \int \frac{d\tau}{\tau} \implies \log(u(\tau)) = \tilde{C} + \log(\tau)$$

which leads to the following solution

$$u(\tau) = C\tau$$

for some arbitrary constant $C = \exp(\tilde{C}) \in \mathbb{R}$ determined by the initial condition. Thus, one way of viewing the solutions to (2.20) is as lines through the origin (Fig 2.4), and these are sometimes also referred to as “rays”.

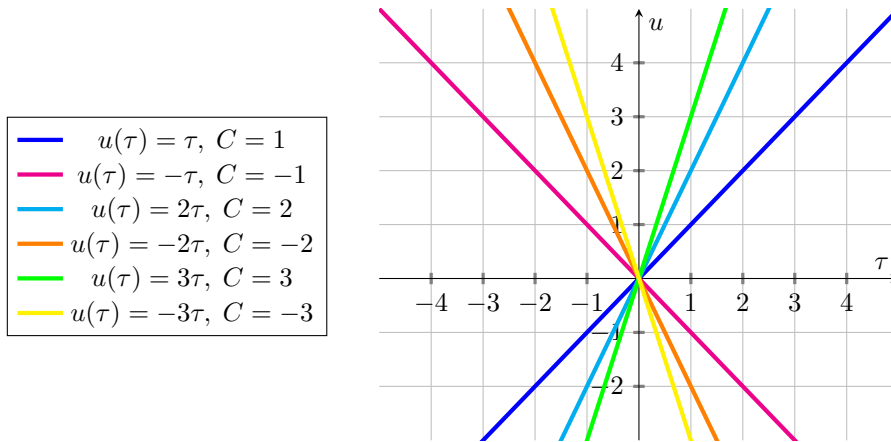


Figure 2.4: Solutions to the ODE $du/d\tau = u/\tau$. We see that the classic rotation mapping as well as reflections through the τ - and u -axes are symmetries of the ODE in question.

Now, it is also possible to study (2.20) from a geometrical perspective by analysing the graph of the solutions. More precisely, we are interested in lines corresponding to sets of points $P \in \mathbb{R}^2$ of the following kind

$$L_C := \left\{ P = \begin{pmatrix} \tau \\ u \end{pmatrix} \in \mathbb{R}^2 : u = C\tau, \text{ for a fixed } C \in \mathbb{R} \right\}$$

and we are then, in general, interested in the entire set of solutions S being the

union of all these lines given by

$$S := \bigcup_{C \in \mathbb{R}} L_C. \quad (2.21)$$

From this perspective it is reasonable to use mathematics from linear algebra and geometry. In introductory courses about vector spaces, one considers various mappings and specifically operators, such as the rotational operator $T_\theta : \mathbb{R}^2 \mapsto \mathbb{R}^2$ defined as

$$T_\theta(P) = T_\theta \left(\begin{pmatrix} \tau \\ u \end{pmatrix} \right) = \begin{pmatrix} \cos(\theta) & -\sin(\theta) \\ \sin(\theta) & \cos(\theta) \end{pmatrix} \cdot \begin{pmatrix} \tau \\ u \end{pmatrix} \quad (2.22)$$

where T_θ rotates the point P counterclockwise with an angle θ . In fact, as the operator T_θ maps planar objects to planar objects, and since the set of solutions in (2.21) covers the whole of \mathbb{R}^2 as the constant C is arbitrary, that is $S = \mathbb{R}^2$, it follows that T_θ maps solutions of (2.20) to other solutions. It is this key property of operators, namely that they preserve the *structure* of the objects they act upon, that is the defining feature of so called *symmetries*. Let us, from now on, adopt the notation by Hydon [45] where symmetries are operators $\Gamma_\epsilon : (\tau, u) \mapsto (\hat{\tau}(\epsilon), \hat{u}(\epsilon))$ where the transformation is a function of the transformation variable $\epsilon \in \mathbb{R}$. Given this notation, the rotation mapping in (2.22) is the following

$$\Gamma_\epsilon^{\text{Rot}} : (\tau, u) \mapsto (\tau \cos(\epsilon) - u \sin(\epsilon), \tau \sin(\epsilon) + u \cos(\epsilon)). \quad (2.23)$$

Two other examples of, perhaps, familiar geometrical transformations are reflections through the τ -axis

$$\Gamma_\epsilon^{\text{Ref}} : (\tau, u) \mapsto (\tau, -u) \quad (2.24)$$

and the *translation* transformation corresponding to translations in the τ -direction

$$\Gamma_\epsilon^{\text{Trans}} : (\tau, u) \mapsto (\tau + \epsilon, u). \quad (2.25)$$

By considering the initial example, it is visually clear (Fig 2.4) that both the rotation mapping in (2.23) and the operator corresponding to reflections through the τ -axis in (2.24) are symmetries of (2.20), while the translations in (2.25) are not. Specifically, a symmetry is a transformation satisfying three conditions

(S1) The transformation preserves structure,

(S2) The transformation is a *diffeomorphism*. More precisely, it is a C^∞ diffeo-

morphism meaning that it is a smooth invertible mapping whose inverse also is smooth,

(S3) The transformation maps the object to itself (e.g. it maps S to S).

It is the third condition (S3), called the *symmetry condition*, that is key for finding the actual symmetries. To generalise this, consider the first order ODE (i.e. $g = v_0 = 0$ in (2.5))

$$\frac{du}{d\tau} = f(u) \quad (2.26)$$

and let S be the set of solution to (2.26). Then, the condition (S3) implies that the symmetry maps solutions of (2.26) to other solutions. Accordingly, it is possible to express the symmetry condition mathematically as follows

$$\frac{d\hat{u}}{d\hat{\tau}} = f(\hat{u}) \quad \text{when} \quad \frac{du}{d\tau} = f(u).$$

Now, since both $\hat{\tau}$ and \hat{u} are functions of the transformations parameter ϵ , the symmetry condition can be expressed more succinctly (by using the chain rule and the total derivative $D_\tau = \partial_\tau + u'\partial_u + u''\partial_{u'} + \dots$) as follows [45]

$$\frac{\partial_\tau \hat{u} + f(\hat{u})\partial_u \hat{u}}{\partial_\tau \hat{\tau} + f(\hat{u})\partial_u \hat{\tau}} = f(\hat{u}). \quad (2.27)$$

It is this condition that defines all symmetries and it is key for finding them.

Moreover, as our initial example illustrated, there are often numerous symmetries to the same ODE. Also, we have that symmetries can be written as combinations of each other since

$$\Gamma_{\pi/2}^{\text{Rot}} \left(\frac{\sqrt{2}}{2}, \frac{\sqrt{2}}{2} \right) = \Gamma_{-\pi}^{\text{Rot}} \left(\Gamma_\epsilon^{\text{Ref}} \left(\frac{\sqrt{2}}{2}, \frac{\sqrt{2}}{2} \right) \right) = \left(-\frac{\sqrt{2}}{2}, \frac{\sqrt{2}}{2} \right)$$

which means that if the point $(\sqrt{2}/2, \sqrt{2}/2)$ is rotated with $\pi/2$ radians counter-clockwise to the point $(-\sqrt{2}/2, \sqrt{2}/2)$ the same result is obtained if the initial point is reflected through the τ -axis and thereafter rotated clockwise with π radians. In fact, the set of symmetries of a given ODE can be classified into a group structure. One says that the infinite set of symmetries Γ_ϵ is an example of a *one parameter Lie group*. This entails that it satisfies the following four conditions

(L1) Γ_0 is the trivial symmetry so that $\hat{t} = t$ and $\hat{y} = y$ when $\epsilon = 0$,

- (L2) Γ_ϵ is a symmetry for every ϵ in the neighbourhood of zero,
- (L3) $\Gamma_\delta \Gamma_\epsilon = \Gamma_{\delta+\epsilon}$ for every δ, ϵ sufficiently close to zero,
- (L4) Each transformed coordinate \hat{t} can be represented as a Taylor series in ϵ (in some neighbourhood of $\epsilon = 0$).

Here, it is also the last condition (L4) which is the most important one as it allows for the construction of a theoretical framework. It is namely the case that the original symmetry condition is typically a non-linear, due to the reaction term f , PDE of two variables τ and u which renders it hard to use. To this end, we make use of the fact that each component of the transformation can be expanded in a Taylor series around $\epsilon = 0$, and using this fact it is possible to simplify the symmetry condition. Before this is done, we will derive a number of useful concepts from the same expansion, and luckily for a first order ODE as in (2.26) these have a geometrical interpretation. It follows that the Taylor series for the Lie group action is [45]

$$\begin{aligned}\hat{\tau} &= \tau + \xi(\tau, u) \cdot \epsilon + \mathcal{O}(\epsilon^2) \\ \hat{u} &= u + \eta(\tau, u) \cdot \epsilon + \mathcal{O}(\epsilon^2)\end{aligned}\tag{2.28}$$

where the tangent to the orbit at (τ, u) is given by the vector \mathbf{v}_1

$$\mathbf{v}_1 = (\xi(\tau, u) \quad \eta(\tau, u))^T = \left(\left. \frac{d\hat{\tau}}{d\epsilon} \right|_{\epsilon=0} \quad \left. \frac{d\hat{u}}{d\epsilon} \right|_{\epsilon=0} \right)^T.\tag{2.29}$$

Similarly, the tangent to the solution travels with with the vector \mathbf{v}_2 (Fig 2.5) defined by

$$\mathbf{v}_2 = (1 \quad u')^T$$

at (τ, u) and using these two vectors it is possible to construct the following matrix

$$M = (\mathbf{v}_1 \quad \mathbf{v}_2) = \begin{pmatrix} 1 & \xi(\tau, u) \\ u' & \eta(\tau, u) \end{pmatrix}.$$

Then, we define the *characteristic* as follows

$$Q(\tau, u, u') = \det(M) = \eta(\tau, u) - u'\xi(\tau, u)$$

and using the fact that $u' = f(u)$ we can define the *reduced characteristic*

$$\bar{Q}(\tau, u) = \det(M) = \eta(\tau, u) - f(u)\xi(\tau, u).$$

This property allows us to mathematically describe the action of a symmetry on a particular solution of an ODE. This follows from the interpretation of the determinant which is the *area of the parallelogram* spanned by the two vectors \mathbf{v}_1 and \mathbf{v}_2 . If it is zero it means that the two vectors (e.g. \mathbf{v}_1 and \mathbf{v}_2) are parallel. Thus, by using the reduced characteristic we can mathematically define the terms an *invariant solution* and the *trivial symmetry* as follows [45]

- $\bar{Q}(\tau, u) = 0 \implies$ The solution is *invariant* under the action of the symmetry meaning that the symmetry maps points to the *same* solution,
- $\bar{Q}(\tau, u) \equiv 0 \implies$ The symmetry is *trivial* implying that all solutions are invariant.

Now, we have arrived at the point where the Taylor expansions in (2.28) can be used to simplify the symmetry condition in (2.27). Thus, what one does is to linearise this condition by substituting the Taylor expansions of $\hat{\tau}$ and \hat{u} into the symmetry condition in order to obtain

$$\frac{f(u) + \epsilon \{ \eta_\tau + f(u)\eta_u \} + \mathcal{O}(\epsilon^2)}{1 + \epsilon \{ \xi_\tau + f(u)\xi_u \} + \mathcal{O}(\epsilon^2)} = f(u + \epsilon\eta + \mathcal{O}(\epsilon^2)).$$

Now, if we further expand each side of the above (or if we multiply both the numerator and denominator with the complement of the denominator “ $1 - \epsilon \{ \xi_\tau + f(u)\xi_u \} - \mathcal{O}(\epsilon^2)$ ”) we obtain

$$f + \epsilon \{ \eta_\tau + (\eta_u - \xi_\tau)f - \xi_u f^2 \} + \mathcal{O}(\epsilon^2) = f + \epsilon \{ \eta f_u \} + \mathcal{O}(\epsilon^2).$$

Lastly, by equating the $\mathcal{O}(\epsilon)$ terms we obtain what is known as the *linearised symmetry condition* [45]

$$\eta_\tau + (\eta_u - \xi_\tau)f - \xi_u f^2 = \eta f_u. \quad (2.30)$$

It is (2.30) that is used in many applications as it is simpler than the original symmetry condition. In fact, it is possible to write (2.30) in terms of the reduced characteristic \bar{Q} . This is true since the following calculations hold

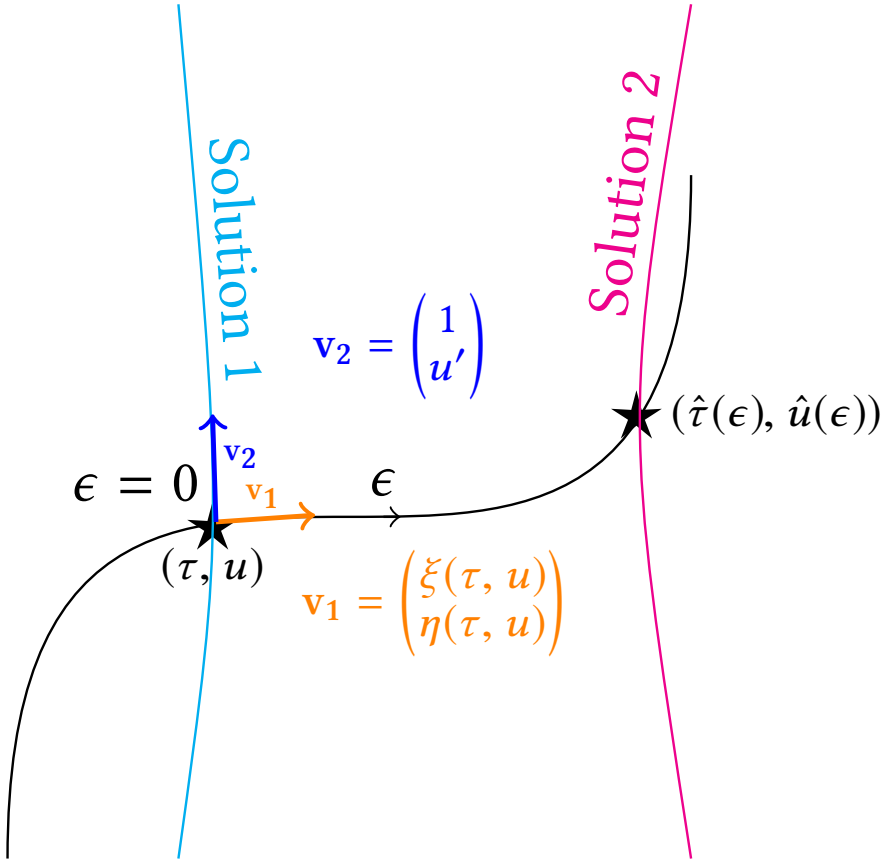


Figure 2.5: The action of a symmetry. The action of the symmetry $\Gamma_\epsilon : (\tau, u) \mapsto (\hat{\tau}(\epsilon), \hat{u}(\epsilon))$ is illustrated. At the point (τ, u) corresponding to $\epsilon = 0$, the tangent vector of the transformation is $v_1 = (\xi(\tau, u) \quad \eta(\tau, u))^T$ while the tangent to the solution travels with the vector $v_2 = (1 \quad u')^T$.

$$\begin{aligned}
& \eta_\tau + (\eta_u - \xi_\tau)f - \xi_u f^2 = \eta f_u \\
\implies & \left[\eta_\tau - \underbrace{\xi_\tau f}_{=\partial_\tau(f\xi)} \right] + \eta_u f - \xi_u f^2 - f\xi f_u = \eta f_u - f\xi f_u \\
\implies & \partial_\tau [\eta - f\xi] + f [\eta_u - (f\xi_u + f_u\xi)] = f_u(\eta - f\xi) \\
\implies & \partial_\tau [\eta - f\xi] + f\partial_u[\eta - f\xi] = f_u(\eta - f\xi).
\end{aligned}$$

and by inserting the reduced characteristic $\bar{Q} = \eta - f\xi$ we obtain

$$\bar{Q}_\tau + f\bar{Q}_u = f_u\bar{Q}.$$

Next, by using the total derivative $D_\tau = \partial_\tau + u'\partial_u = \partial_\tau + f\partial_u$ we see that the left hand side above can be rewritten as follows

$$D_\tau\bar{Q} = f_u\bar{Q}. \quad (2.31)$$

This is the linearised symmetry condition in terms of the reduced characteristic \bar{Q} , and it is important to emphasise that (2.30) and (2.31) are equivalent.

Furthermore, a key concept within symmetry methods is that of the *canonical coordinates*. These are coordinates $(r, s) = (r(\tau, u), s(\tau, u))$ on which symmetries have a particularly simple action, namely symmetries merely translate the canonical coordinates in the s -direction (recall the translation symmetry $\Gamma_\epsilon^{\text{Trans}}$ in (2.25))

$$(\hat{r}, \hat{s}) = (r, s + \epsilon).$$

From a linear algebra point of view, this corresponds to a change of coordinates with the following property

$$\begin{pmatrix} r_t & r_y \\ s_t & s_y \end{pmatrix} \begin{pmatrix} \xi(\tau, u) \\ \eta(\tau, u) \end{pmatrix} = \begin{pmatrix} 0 \\ 1 \end{pmatrix}.$$

The characteristic equations to find the s -coordinate are [45]

$$\frac{d\tau}{\xi(\tau, u)} = \frac{du}{\eta(\tau, u)} = ds$$

where the r -coordinate is a *first integral* of the following ODE [45]

$$\frac{du}{d\tau} = \frac{\eta(\tau, u)}{\xi(\tau, u)}$$

and r is thus found by solving the above ODE. Usually, one starts by finding $r = r(\tau, u)$ as a function of the original coordinates and then the s coordinate is obtained by one of the characteristic equations above, for example [45]

$$s = \left(\int \frac{d\tau}{\xi(\tau, u(r, \tau))} \right) \Big|_{r=r(\tau, u)}.$$

The canonical coordinates can be used to find solutions of ODEs as well as finding the symmetries themselves, and thus a key step in symmetry methods is to transform the original coordinates (τ, u) to the canonical counterparts. Using these coordinates, it is now possible to define the concept of a generator which allows us to generalise the framework.

Utilising the tangents in combination with the canonical coordinates, we can now develop a rigorous methodology for finding symmetries. This can be achieved by using the following partial differential operator

$$X = \xi(\tau, u)\partial_\tau + \eta(\tau, u)\partial_u \quad (2.32)$$

which is called the *infinitesimal generator of the Lie group*. As we will soon show, this can be used to generate the Lie group, that is to generate the symmetries. A particular appealing property of the canonical coordinates is that this generator reduces to

$$X = \partial_s = \frac{\partial}{\partial s}. \quad (2.33)$$

Now, consider the transformation $\hat{\tau}$ and imagine that it can be rewritten in canonical coordinates using the smooth and infinitely continuously differentiable function F as follows

$$\tau = F(s, r) \iff \hat{\tau} = F(\hat{s}, \hat{r}).$$

Then, by applying Taylor's theorem to expand F , we obtain

$$\begin{aligned}\hat{\tau} &= F(\hat{s}, \hat{r}) = F(s + \epsilon, r) = \sum_{j=0}^{\infty} \frac{\epsilon^j}{j!} \underbrace{\frac{\partial^j}{\partial s^j}}_{=X^j} (F(s, r)) \\ &= \underbrace{\sum_{j=0}^{\infty} \frac{\epsilon^j}{j!} X^j}_{e^X} F(s, r) = e^X F(s, r) = e^X \tau\end{aligned}$$

where we in the last step define the *exponential map*

$$e^X = \sum_{j=0}^{\infty} \frac{\epsilon^j}{j!} X^j.$$

Thus, the symmetries are generated by the infinitesimal generator X using the exponential map as follows

$$\hat{\tau} = e^X \tau \quad (2.34)$$

$$\hat{u} = e^X u. \quad (2.35)$$

Note here that X is a differential operator, and thus the meaning of the terms “ X^j ” for an arbitrary index j is not to “take the j^{th} power of X ” but rather to apply X , which is the generator, j times in a recursive manner. It is this generator that allows us to generalise the symmetry framework to higher order ODEs and thereby systems of ODEs.

Consequently, consider a higher order ODE of the following form

$$u^{(n)} = f(u, u', \dots, u^{(n-1)}), \quad u^{(k)} = \frac{d^k u}{d\tau^k}. \quad (2.36)$$

Thus, we are interested in symmetries of the following kind

$$\Gamma_{\epsilon} : (\tau, u, u', \dots, u^{(n)}) \mapsto (\hat{\tau}, \hat{u}, \hat{u}', \dots, \hat{u}^{(n)})$$

where

$$\hat{u}^{(k)} = \frac{d^k \hat{u}}{d\hat{\tau}^k}, \quad k = 1, \dots, n.$$

Note that, in similarity to the case of first order ODEs, the symmetries for higher order ODEs can be understood from a geometrical perspective. In other words, the ODE in (2.36) defines a high dimensional geometrical object called

a *manifold* [45, 79] in \mathbf{R}^{n+1} where each derivative $u^{(k)}$ can be thought of as a spatial direction⁴². In this high dimensional and general context, it is hard to use intuition in order to grasp the meaning of the various concepts and for an interpretation of the various concepts it is advised to refer back to the planar case (τ, u) corresponding to the geometrical view of the first order ODEs in (2.26). Interestingly enough, the solution $u(\tau)$ of (2.36) from a function perspective is the projection of $(\tau, u, u', \dots, u^{(n)})$ onto the (τ, u) -plane.

To formulate the linear symmetry condition, we remind ourselves that the derivatives of the symmetries are determined by

$$\hat{u}^{(k)} = \frac{d\hat{u}^{(k-1)}}{d\hat{\tau}} = \frac{D_\tau \hat{u}^{(k-1)}}{D_\tau \hat{\tau}}, \quad \hat{u}^{(0)} \equiv \hat{u}$$

where the total derivative is defined as $D_\tau = \partial_\tau + u' \partial_u + u'' \partial_{u'} + \dots$. Then, we define the symmetry condition for a higher order ODE as follows

$$\hat{u}^{(n)} = f(\hat{u}, \hat{u}', \dots, \hat{u}^{(n-1)}) \quad \text{when (2.36) holds.} \quad (2.37)$$

Again, we can calculate the Taylor expansions of the transformations as follows

$$\begin{aligned} \hat{\tau} &= \tau + \epsilon \xi + \mathcal{O}(\epsilon^2) \\ \hat{u} &= u + \epsilon \eta + \mathcal{O}(\epsilon^2) \\ \hat{u}^{(k)} &= u^{(k)} + \epsilon \eta^{(k)} + \mathcal{O}(\epsilon^2), \quad k \geq 1. \end{aligned}$$

Then, substituting the corresponding linearisations into (2.37) and then setting the $\mathcal{O}(\epsilon)$ terms equal yields the *linearised symmetry condition*

$$\eta^{(k)} = \xi \omega_\tau + \eta \omega_u + \eta^{(1)} \omega_{u'} + \dots + \eta^{(n-1)} \omega_{u^{(n-1)}} \quad \text{when (2.36) holds.} \quad (2.38)$$

The functions $\eta^{(k)}$ are calculated recursively and it is possible to show [45] that all these terms can be calculated using the so called *prolongation formula*

$$\eta^{(k)}(\tau, u, u', \dots, u^{(k)}) = D_\tau \eta^{(k-1)} - u^{(k)} D_\tau \xi. \quad (2.39)$$

Again, these derivatives are calculated in a recursive fashion. Also, it is possible to expand the notion of a generator by introducing the *prolonged infinitesimal generator*

$$X^{(n)} = \xi \partial_\tau + \eta \partial_u + \eta^{(1)} \partial_{u'} + \dots + \eta^{(n)} \partial_{u^{(n)}}$$

⁴²For a more rigorous exposition on the theory of differential geometry and the application of Lie groups to differential equations, see [79].

and using this formula we can reformulate the linearised symmetry condition as follows [45]

$$X^{(n)}(u^{(n)} - f(u, u', \dots, u^{(n-1)})) = 0 \quad \text{when (2.36) holds.}$$

Moreover, let $\tilde{\mathcal{L}}$ denote the set of all infinitesimal generators of one-parameter Lie groups of point symmetries of an ODE of order $n \geq 2$. Now, since the linearised symmetry condition is linear in ξ and η and so

$$X_1 + X_2 \in \tilde{\mathcal{L}} \implies c_1 X_1 + c_2 X_2 \in \tilde{\mathcal{L}}, \quad \forall c_1, c_2 \in \mathbb{R}.$$

Therefore, $\tilde{\mathcal{L}}$ is a vector space. *The dimension of this vector space is the number of arbitrary constants that appear in the general solution to the linearised symmetry condition [45].* Consequently, every $X \in \tilde{\mathcal{L}}$ can be written as $X = \sum_{i=1}^R c_i X_i$ for $c_i \in \mathbb{R}$ where $\{X_1, \dots, X_R\}$ is a basis of $\tilde{\mathcal{L}}$. At this point, it is reasonable to pose the question of how higher order ODEs as in (2.36) relate to systems of ODEs which is the focus of this thesis?

In fact, all systems of ODEs can be written as a higher order ODE and vice versa. To exemplify this, consider the second order ODE from elementary mechanics in the context of damped oscillations in a spring

$$\underbrace{mx''}_{\text{Newton's 2nd law}} = - \underbrace{bx'}_{\text{Damping force}} - \underbrace{kx}_{\text{Hooke's law}}.$$

The solution $x(t)$ describes the position of a mass, e.g. a weight, which through a spring is (vertically) attached to a rigid support, e.g. the roof, and this solution is a function of the time t . By introducing the pseudo-state $y = x'$ we can write this as the following matrix system

$$\frac{d}{dt} \begin{pmatrix} x \\ y \end{pmatrix} = \begin{pmatrix} 0 & 1 \\ -\frac{k}{m} & -\frac{b}{m} \end{pmatrix} \begin{pmatrix} x \\ y \end{pmatrix}.$$

This holds true in general as well, as any higher order ODE

$$u^{(n)} = f(u, u', u'', \dots, u^{(n-1)})$$

can be converted into a n -dimensional system of ODEs as follows

$$\begin{aligned} u'_1 &= u_2 \\ u'_2 &= u_3 \\ &\vdots \\ u'_{(n-1)} &= u_n \\ u'_n &= f(u_1, u_2, u_3, \dots, u_{n-1}, u_n). \end{aligned}$$

This demonstrates that the theory concerning symmetry methods for higher order ODEs also describes the symmetries of systems of ODEs which is the focus of this thesis. The geometrical interpretation of symmetries for a higher order ODE as in (2.36) is that each derivative $y^{(k)}$ corresponds to a “spatial direction” in a high dimensional manifold. Accordingly, as the states in a system of ODEs correspond to a derivative in a higher order ODE, this implies that the various states of a system of ODEs can also be viewed, from a geometrical point of view, as a “direction” in a high dimensional manifold corresponding to the state space. On this note, this allows us to summarise the entire background by introducing the last concept which is a theoretical version of the identifiability analysis described in subsection 2.2.5 in the light of this geometrical perspective of differential equations.

2.2.7 Structural identifiability (SI)

Now, we return to the concept of identifiability which was introduced in subsection 2.2.5. To this end, consider the model in (2.13) on page 30 with the output \hat{y} and initial conditions u_0 and v_0 respectively given by

$$\begin{aligned} \frac{du}{d\tau} &= f(u(\tau), v(\tau), \theta) \\ \frac{dv}{d\tau} &= g(u(\tau), v(\tau), \theta) \\ \hat{y}(\tau, \theta) &= o(u(\tau), v(\tau), \theta) \\ u(0) &= u_0 \text{ and } v(0) = v_0. \end{aligned}$$

Recall, that we are interested in the following question: given the observed output \hat{y} and the initial conditions (u_0, v_0) which parameters in the parameter vector $\theta \in \mathbb{R}_+^p$, $p \in \mathbb{N}_+$ can be identified? In this theoretical scenario, no time

series is available, and the properties of the system that can be considered to be “known” are the initial conditions u_0 and v_0 as well as the kinetic parameters θ . Now, in order to answer the previously posed question theoretically in the absence of data, the *time evolution* of the output \hat{y} is required.

In the context of the geometrical perspective, it is possible consider the *phase portrait*, which is the state space determined by (u, v) , as a (two dimensional) manifold. Given this notation, the generator of the *time evolution* of the system in (2.13), analogous to the infinitesimal generator of the Lie group in the context of symmetry methods, is the following

$$X = f \frac{\partial}{\partial u} + g \frac{\partial}{\partial v}.$$

Using this operator, the derivative of any order of the states $u(\tau)$ and $v(\tau)$ can be expressed according to

$$\left. \begin{aligned} u^{(j)}(0) &= X^j f(u, v, \theta) \Big|_{u=u_0, v=v_0} \\ v^{(j)}(0) &= X^j g(u, v, \theta) \Big|_{u=u_0, v=v_0} \end{aligned} \right\}, \quad j \in \{1, \dots, \infty\}$$

which are the terms in a Taylor expansion around $\tau = 0$ corresponding to the (known) point (u_0, v_0) in the phase portrait given by the initial conditions. Similarly, the time evolution of the output \hat{y} is determined by this operator is

$$\hat{y}^{(j)}(0) = X^j o(u, v, \theta) \Big|_{u=u_0, v=v_0}, \quad j \in \{1, \dots, \infty\} \quad (2.40)$$

and it is this equation that is key in structural identifiability analysis. In other words, the derivatives $\hat{y}^{(j)}$ in (2.40) completely determine the time evolution of the output \hat{y} close to the time $\tau = 0$ and accordingly identifiability analysis is based on solving the equations in (2.40). However, as the Taylor expansion is infinite, there are infinitely many equations to solve in (2.40) which, of course, is an impossible task to accomplish. Luckily, it has been shown that only the first $\nu = n + p - 1 = p + 1$, where $n = 2$ is the number of states and p is the number of parameters, equations in (2.40) must be solved in order to determine the evolution of \hat{y} locally around $\tau = 0$. This is on account of the fact that all of the higher order derivatives can be algebraically expressed in terms of the first ν derivatives [4, 99].

Accordingly, we can gather all the first ν derivatives $\hat{y}^{(j)}(0)$, $j \in \{1, \dots, \nu\}$ in a column vector [53] denoted \mathcal{Y} given by

$$\mathcal{Y} = \mathcal{Y}(u_0, v_0, \theta).$$

Then, the task could be re-formulated as calculating \mathcal{Y} provided that the initial conditions u_0 and v_0 as well as the parameters θ are known. Again, it is worth noting that the parameters (as well as the states) are included as “dimensions” in the geometrical context as we are interested in investigating whether or not certain parameters in θ can be identified with the observed output \hat{y} uniquely determined by \mathcal{Y} . Given this setting, the so called *rank test for structural identifiability* [84] states that the vector \mathcal{Y} can be uniquely calculated *if and only if* the Jacobian matrix⁴³

$$J(u_0, v_0, \theta) = \left. \frac{\partial \mathcal{Y}(u, v, \tilde{\theta})}{\partial (u, v, \tilde{\theta})} \right|_{u=u_0, v=v_0, \tilde{\theta}=\theta} \quad (2.41)$$

has full rank [53]. Note that the Jacobian matrix corresponds to the first term in the Taylor expansion, where the parameters “ $\tilde{\theta}$ ” are included as “dimensions”, of \hat{y} around $\tau = 0$. Moreover, this matrix has full rank if its columns are *linearly independent* and the entries of the Jacobian matrix are given by [53]

$$\begin{aligned} & \left. \frac{\partial}{\partial u} X^i o(u, v, \tilde{\theta}) \right|_{u=u_0, v=v_0, \tilde{\theta}=\theta}, \quad \left. \frac{\partial}{\partial v} X^i o(u, v, \tilde{\theta}) \right|_{u=u_0, v=v_0, \tilde{\theta}=\theta} \quad \text{and} \\ & \left. \frac{\partial}{\partial \tilde{\theta}_j} X^i o(u, v, \tilde{\theta}) \right|_{u=u_0, v=v_0, \tilde{\theta}=\theta}, \quad \text{for } j \in \{1, \dots, p\}, i \in \{1, \dots, \nu\}. \end{aligned}$$

where the function o determines the output \hat{y} . If the Jacobian has full rank, the model is referred to as structurally identifiable and thus this defines the concept of *structural identifiability (SI)*.

Interestingly, the concept of SI can be understood similarly to the interpretation of the sensitivities in (2.18) in the context of NI. As previously described, if a sensitivity “ $\partial \hat{y} / \partial c_i$ ” is small for a certain parameter c_i within NI-analysis, then this parameter will not be possible to identify with the observed data \hat{y} . Analogously, this is what the entries of the Jacobian matrix in (2.41) captures as well but in the context of SI. In fact, the connection between SI and NI is straightforward: SI can be thought of as NI when the errors between the observed and simulated outputs vanish, i.e. in the limit $e_i = y_i - \hat{y}_i \rightarrow 0 \forall i \in \{0, \dots, N\}$ in (2.14) on page 31. In other words, SI corresponds to a situation without noise where the output \hat{y} is completely determined by the function

⁴³Note that this is a slightly different Jacobian matrix than that encountered in linear stability analysis, see subsection 2.2.3.

o. Therefore, a model as in (2.13) on page 30 that is structurally identifiable can still turn out not to be numerically identifiable, while if a model is not numerically identifiable it can never be structurally identifiable (Fig 2.6).

Another interesting observation from the Jacobian matrix (2.41), is that it can be used for reducing large models. In a situation with many more states, i.e. more proteins than just u and v , the derivatives with respect to all states are included in the Jacobian matrix and thereby contributing to the identifiability analysis. By identifying which states, denote these u_i , that do not change the output, i.e. small values of " $\partial \mathcal{Y} / \partial u_i$ ", it is possible to remove these from the model in order to reduce it.

In practice, it is common to start with an analysis of the SI of a model before proceeding with the NI. In fact, it is even advisable to investigate the SI before the data is collected as such an analysis can indicate which parameters that can be estimated with the given output from a theoretical perspective. In this way, the SI analysis can be part of the experimental design before the model validation, PE and NI analysis are conducted.

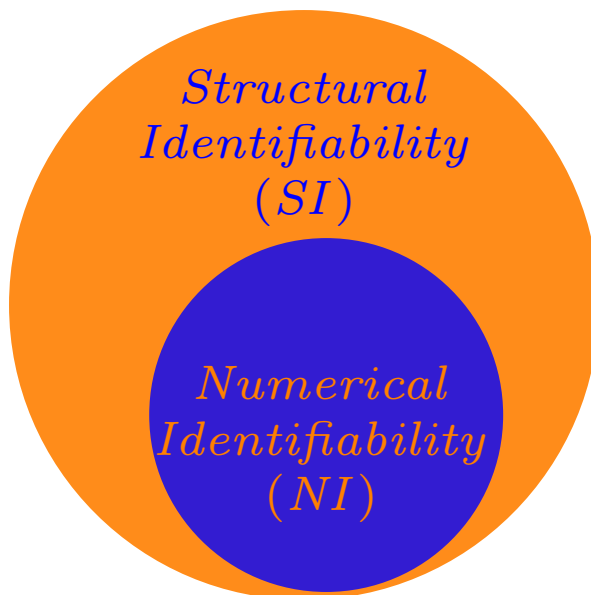


Figure 2.6: The relation between *structural identifiability, SI, and numerical identifiability, NI*. The set of numerically identifiable models is a subset of the set of structurally identifiable models.

3 Large time scale: Modelling of the entire life span of budding yeast on a single cell and population level

Mathematical modelling of unicellular ageing has been successfully implemented. Specifically, certain models of particular interest describe the accumulation of damage as a consequence of cell growth, they include the counter measures of repair and degradation and they involve the retention of damage as well as the degree of asymmetry in the cell division. In Paper II, we constructed such a model that simulated the entire life span of single yeast cells and a novelty here was that the RLS of individual cell was calculated. This allowed us to quantify, using simulations, the effect of changing the previously mentioned properties, e.g. the formation, repair and retention of damage, on the RLS. Also, we derived three theoretical results under the assumptions that a cell needs a minimum amount of functioning proteins in order to live. These were a theoretical upper limit on the maximum degree of asymmetry with which a cell can divide, that symmetrically dividing cells such as bacteria cannot retain damage and we derived an upper bound on the maximum proportion of damage that a mother cell can retain as a function of its resilience to damage. In this chapter, we focus on a small aspect of this article concerning the model validation using experimental data as this is an overall theme of the thesis.

Moreover, using this type of framework it is possible to simulate the distribution of damage among vast numbers of cells in order to elucidate strategies that can improve the overall fitness of the population. More precisely, these models allow for the systematic investigation of the precise effect on the population

fitness of changing individual forces such as an increase in the capacity to retain damage and an example of such a population level analysis is conducted in Paper III. In addition, these large scale simulations can be run for multiple generations enabling the evolutionary study of damage accumulation. It is worth noting that this is currently not possible or at least highly complicated as well as time consuming to study experimentally which makes the prospects of this type of modelling particularly appealing.

In order to cope with the large time scales as well as the vast number of cells, the structure of these models is rather simple. Within this framework, each cell is assumed to consist of merely two components, namely intact proteins P and damage D , implying that these models view the cell from a holistic perspective where the processes involved in the overall cellular activity are simplified. In other words, the level of detail where it is possible to describe the dynamics of specific proteins is sacrificed for the capacity to model the entire life span of single cells as well as studying whole populations. The dynamics of the accumulation of damage is determined by the ODE-model in (3.1)

$$\begin{aligned}
 \frac{dP}{d\tau} &= f(P, D, \theta, \tau) \\
 \frac{dD}{d\tau} &= g(P, D, \theta, \tau) \\
 P(0) &= f_P(s, \text{re}) \\
 D(0) &= f_D(s, \text{re}) \\
 \hat{y}(\theta, \tau) &= P(\theta, \tau) + Q D(\theta, \tau).
 \end{aligned} \tag{3.1}$$

Here, the non-linear reaction terms f and g respectively determine the formation of intact proteins and damage where the kinetic rate parameters are gathered in the vector θ . Furthermore, there are two functions which determine the initial concentrations, namely f_P for the intact proteins and f_D for the damage. These depend on two parameters, the size proportion $s \in [1/2, s_{\max}]$ for $s_{\max}(Q) \in (1/2, 1)$ which determines whether the cell divides symmetrically, e.g. $s = 1/2$, or asymmetrically, $s > 1/2$, and the retention coefficient $\text{re} \in [0, \text{re}_{\max}(s, Q, D)]$ for $\text{re}_{\max}(s, Q, D) \in (0, 1)$ corresponding to the proportion of damage that the mother cell retains. Another key property is the parameter Q corresponding to the resilience to damage of an individual cell which is the amount of damage that a cell can cope with before undergoing cell death. This parameter determines the upper bound on the size proportion $s_{\max}(Q)$, the upper bound on the retention coefficient $\text{re}_{\max}(s, Q, D)$ and it can also be interpreted, from an empirical point view, as the increase in volume

of an individual cell over the course of its lifespan. This follows from the fundamental assumption of the model (i.e. that the cell merely consists of intact proteins and damage) stating that the total protein content, denoted by $\hat{y} = P + QD$, is proportional to the volume of the cell. Now, as an increase in cell size is indicative of ageing in yeast cells it is possible using this output to validate and possibly select among candidate models using experimental data as is described in Paper II.

To select among candidate models, the models were fitted to time series data of the size of the cell (Tab 3.1). To obtain the ageing aspect of the validation procedure, the models were fitted to an ‘‘average’’, in the sense that a statistical average of multiple growth curves were used, yeast cell both when it was young¹ and when it was old². The three candidate models that were calibrated to the measured data was our model in Paper II compared to the models in [25] and [16].

Table 3.1: Candidate models of damage accumulation. The reaction terms f and g in (3.1) as well as the fit in terms of the least square LS to the experimental data is displayed. The compared models are our model in Paper II, the model in [25] and the model in [16].

Model	$f(P, D, \theta, \tau)$	$g(P, D, \theta, \tau)$	LS(θ)
Paper III	$P(g - D) - k_1P + k_2QD$	$(k_1/Q)P - k_2D$	0.20
Erjavec et al.	$\alpha \left(\frac{P}{K_M + P + QD} \right) - k_1P$	$\frac{k_2}{Q}P - k_3D$	0.46
Clegg et al.	$(1 - \beta)P \left(\frac{P}{P + QD} \right) - k_1P + k_2D \left(\frac{P}{\beta P + QD} \right)$	$\frac{k_1}{Q}P - \frac{\beta}{\mu}D \left(\frac{P}{\beta P + QD} \right)$	0.43

Consequently, our model would be favoured over the rivals which we conclude in Paper II. Not only is the fit in terms of the least square value LS(θ) lower but also the model structure is much simpler both in terms of the number of

¹By young we mean damage free daughter cell.

²By old we mean a mother cell growing until the last cell division before cell death occurs.

parameters as well as the complexities of the non-linearities. Thus, the model in Paper II is both simple in terms of the structure and it describes the experimental data well which motivated further investigation of the model. However, despite the fact that our model is selected based on the statistical guidelines, it is not evident that it is the correct description of damage accumulation.

Although one of the three candidates describes the data best, there is no guarantee that it actually is correct. First of all, the output \hat{y} in (2.5) measures the increase in size over time indicating that a model that fits the data well has the ability to replicate a growth curve which in fact all three models have, at least from a visual perspective, since the models can capture the trend in the data (see Fig S3 in the supplementary material of Paper II). In the context of ageing, this entails that the other more crucial parameters corresponding to formation and repair of damage do not affect the model calibration significantly which is reflected in the low *numerical identifiability*, NI³, of these parameters (see Tab S3 in the supplementary material of Paper II). One way to improve the identifiability is to alter the observed output and, in this specific case, a suitable candidate would be to follow a damage marker over time which would correspond to the output $\hat{y}(\theta, \tau) = D(\tau)$. Even if a change of output⁴ ameliorates the identifiability of the ageing related parameters, it is still possible that there exists a fourth candidate model structure, i.e. two additional functions f and g respectively, that would yield a better fit to the data than the presented candidates (Tab 3.1). The situation described above is fairly common in mechanistic modelling especially within systems biology where a good fit to experimental data can give modellers a false sense of security regarding the model structure. An undesirable consequence of validating or selecting a faulty mechanistic model, is that it can subsequently be used for extrapolation in terms of forecasting novel outcomes.

By selecting the wrong mechanistic model, false predictions regarding unicellular ageing can be drawn. To this point, the previously described candidate models (Tab 3.1) make fairly different predictions regarding how the RLS is changed due to a change in the resilience to damage of an individual yeast cell (see Fig S4 in the supplementary material of Paper II). In fact, all the predictions regarding strategies for prolonging the RLS of individual cells made in Paper II as well as the analytical results should be interpreted as indications⁵ or hypotheses rather than statements of facts. Similarly, the same conclusion extends

³If a parameter has low NI, we mean that this parameter does not influence the simulated output \hat{y} . Accordingly, the value of this parameter can be set to any value based on the measured data and it is therefore not identifiable.

⁴A crucial improvement would also be the *addition* of outputs, e.g. $\hat{y}_1, \dots, \hat{y}_i, i \in \mathbb{N}_+$.

⁵That is various claims should *always* be read as follows "Under the assumption that the model is true, we see that...".

to the simulations (using the model in Paper II as a basis) on the population level presented in Paper III where strategies to increase the overall population fitness are investigated by altering the involved parameters. This problem links back to the initial discussion of this chapter about using models as a means to simulate population level aspects of ageing in an evolutionary context. On account of the difficulty of constructing, validating and selecting the "true" mechanistic model combined with the fact that the large scale simulations of the damage accumulation models are hard to validate, the predictions of these models should be viewed as hypotheses or suggestions rather than undisputed evidence.

The presented modelling framework consists of an overview picture of unicellular ageing but it lacks chemical details of specific proteins. In other words, these models describing the dynamics of bulk proteins involve the major forces including cell growth as well as formation, degradation, repair and retention of damage but the framework cannot account for kinetic reaction rates of individual proteins involved in any of these larger processes. To this end, the focus of the thesis will subsequently be "zoomed-in" on a detailed reaction scheme within the first phase of the cell division in budding yeast.

4 Short time scale: Modelling of Cdc42 mediated cell polarisation in budding yeast

The fascination of modelling the dynamics of Cdc42 comes from a particularly intriguing phenomena [15, 20, 21, 32, 34, 35, 49, 50, 61, 71, 81, 95, 107, 109]. More precisely, the concentration profile of the active component of Cdc42, which evolves inhomogeneously, is modelled by *diffusion driven instability* [75] originally proposed by Alan Turing [108]. Given a spatiotemporal RD model composed of a coupled system of PDEs, it is possible to simulate the aggregation of active Cdc42 at a specific spatial location called the *pole*¹ over time. However, as spatial models are not part of the classic systems biology cycle entailing the validation of model predictions using data, the results of these models often given by a linear stability analysis combined with simulations are highly difficult to validate. Also, as PDEs are generally more complex to analyse than ODEs, these models often approximate the spatial domain by a one-dimensional line, which further complicates the task of interpreting the obtained results as the geometric description of the cell is too simple. To generate more realistic models, newer attempts have included a three-dimensional spatial description of the cell where both the cytosol and the membrane are included.

In Paper IV, we developed a model of Cdc42-mediated cell polarisation which is realistic in two respects. On the one hand, the underlying reaction scheme is well-motivated by the literature where each parameter has a clear meaning in terms of biology and on the other hand the description of the morphology of the cell adds to its validity. On the latter point, the implemented mathematical framework belongs to a relatively new class of RD models called the *bulk-*

¹The *pole* is where the new cell grows out, i.e. the location of the bud in *S.cerevisiae*.

surface models [17, 87, 88]. Here, the geometry of the cell is described by a three-dimensional ball whose interior corresponds to the cytosol and where the two-dimensional surface, i.e. the sphere, corresponds to the membrane. In addition, the cytosol is viewed as a bulk in which the cytosolic GDI-bound component of Cdc42 diffuses and through transfer reactions the system is further coupled to the membrane where the reactions governing activation and inactivation of Cdc42 occur. Moreover, as the linear stability analysis of diffusion driven stability has been generalised to this more realistic geometrical description [87, 88] it is possible to derive analytical results which can be used to guide the simulations. To this end, we ensured appropriate stability properties of our model by means of a mathematical theorem and conducted a thorough investigation of the parameter space in order to map out various types of diffusion-driven instability in terms of the kinetic parameters. Besides, as the use of this type of modelling is not widespread, it has not been implemented in a systematic fashion to investigate the effect of model parameters on cell polarisation.

Since spatial data with high resolution is lacking, the study of cell polarisation is highly dependent on spatiotemporal simulations. In the case of the three-dimensional bulk-surface models, this requires high performance algorithms to be able to solve these RD equations efficiently, especially if the aim is to render the simulations more quantitative. Thus far, the bulk-surface models have focused more on capturing the qualitative behaviour of cell polarisation using simulations which entails the formation of an inhomogeneous concentration profile of Cdc42 where the active state forms a pole. This is often achieved by running the simulations with kinetic rate parameters satisfying the Turing conditions for *diffusion driven instability* [75] and often merely a few simulations are run to validate that a pole evolves. To render this kind of simulations more quantitative where the effect of altering individual rate parameters such as the activation rate of GAP² on the polarisation process, an efficient algorithm for solving the RD system is required. To this end, we developed an algorithm combining *Finite Differences (FD)* in time and the *Finite Element Method (FEM)* in space which generated the spatiotemporal simulations of cell polarisation. To increase the performance, this combined FD-FEM approach uses an adaptive step size in time and it also contains a termination criteria which stops when a pole is formed. The latter part of the program enables us to measure specific properties such as the time to polarisation, the area of the pole and the maximum concentration of active Cdc42 in the pole which thus produces much more quantifiable simulations. In a sense, these spatiotemporal simulations replace the function of the time series data in Chapter 3 where the desired result is to form a single pole as oppose to some other type of “pattern” in the

²For more information on the activation of Cdc42, see the background in section 2.1.3.

concentration profile and it is this that is used as a validation of the models.

In Paper IV, we set out to formulate a quantitative formulation of Cdc42-mediated cell polarisation. The structure of the model, originally proposed in [87], is the following

$$\begin{aligned}
 \frac{\partial V}{\partial \tau} &= D\Delta V, & \mathbf{x} \in \Omega, t \in \mathbb{R}_+ \\
 -D [(\nabla V)^T \mathbf{n}] &= \gamma q(u, v, V), & \mathbf{x} \in \Gamma, t \in \mathbb{R}_+ \\
 \left. \begin{aligned}
 \frac{\partial u}{\partial \tau} &= \gamma f(u, v) + \Delta_\Gamma u \\
 \frac{\partial v}{\partial \tau} &= \gamma (-f(u, v) + q(u, v, V)) + d\Delta_\Gamma v
 \end{aligned} \right\}, & \mathbf{x} \in \Gamma, t \in \mathbb{R}_+.
 \end{aligned} \tag{4.1}$$

In (4.1), Ω corresponds to the cytosol and Γ corresponds to the membrane. The three states are the cytosolic GDI-bound Cdc42 V , the inactive GDP-bound Cdc42 v and the active GDT-bound Cdc42 u where the last two states are restricted to the membrane.

Moreover, the reactions are determined by the two non-linear functions q and f respectively. The cytosolic flux to the membrane as well as the dissociation from the membrane to the cytosol is determined by the function q . The reactions occurring in the membrane corresponding to the activation and inactivation of Cdc42 are determined by the function f . As we can see, the former function q is *almost*³ the same in both models in Tab 4.1 while the latter function f is substantially simpler in our model compared to the one in [87, 88]. As argued for in Paper IV, this simpler model structure is not only more biologically realistic in addition to having easily interpretable parameters but from a model selection perspective it is preferable due to its relative simplicity. Hence, if our model can generate biologically realistic simulations it could be argued that it should be favoured over the alternative model.

³The function q is the same but the non-dimensionalisation procedure differs between the two models. The states in the model in [87, 88] are scaled by the parameter c_{\max} and thus this parameter is not present in the dimensionless version of the model. In our model in Paper IV, we use another non-dimensionalisation related to the one used in [96].

Table 4.1: Candidate models of Cdc42-mediated cell polarisation. The reaction terms f and q in (4.1). The compared models are our model in Paper IV and the model by Rätz and Röger [87, 88]

Model	$f(u, v)$	$q(u, v, V)$
Paper IV	$c_2v - u + u^2v$	$c_1V(c_{\max} - (u + v)) - c_{-1}v$
Rätz and Röger	$\left(a_1 + (a_3 - a_1)\frac{u}{a_2+u}\right)v - a_4\frac{u}{a_5+u}$	$c_1V(1 - (u + v)) - c_{-1}v$

Our model in Paper IV reliably produces biologically realistic simulations in terms of a single pole of active Cdc42, u . These results are qualitatively similar for different sets of kinetic parameters while quantitative measures such as the time to polarisation and the size of the pole differ. In the given situation where data is lacking, it is possible to argue for the selection of our model as it can reproduce the qualitative behaviour of Cdc42 and its structure is simpler than the other candidate. However, there is of course even larger difficulties regarding differentiating between the alternative mechanisms in this situation compared to the situation of the RLS models in Chapter 3 where times series data was available. Also, the two different mechanisms encoded in the respective models probably answer detailed questions differently. These questions can, for example, be how a specific decrease in the efficiency of the GEFs, reflected in the parameters a_1 and c_2 respectively, affects properties such as the polarisation time.

In summary, a reoccurring problem in mechanistic modelling both on the short (Chapter 4) and the long (Chapter 3) time scale is the validation of models. An attempt to tackle this problem is described in the subsequent chapter which describes a mathematical tool called *symmetry methods*, see subsection 2.2.6, in the context of constructing mechanistic models.

5 Towards the key to understanding complex biological systems: symmetries in the construction of mechanistic models

Thus far, we have established that there exists no unambiguous way of constructing and validating mechanistic models. Currently, the statistical criteria¹ states that the description with the least number of assumptions that best describes the data is in some sense reasonable. The underlying fairly *old*² philosophical principle behind this model selection criteria is perhaps most famously known as *Occam's razor* [41] originally formulated as “do not multiply entities beyond necessity”. Later, a succinct reinterpretation of this proposition was made by the physicist Albert Einstein [86]

“Everything should be made as simple as possible, but not simpler.”

Throughout the history of science this doctrine has been implemented, and to highlight its importance let us consider an anecdote³ from the encounter between the physicist *Pierre-Simon de Laplace*⁴ and the french emperor Napoleon

¹For the details of the statistical criteria, see (2.19) on page 35.

²In fact, the principle is medieval. Further, it is named after the English philosopher and theologian William of Ockham (sometimes spelled Occam).

³See [41] for a more exhaustive description of the story of Laplace and the emperor Napoleon.

⁴Yes, this is the same physicist who has given name to the Laplace operator in the reaction diffusion models, see (2.6) on page 22.

Bonaparte. When Laplace presented his model of the solar system the inquisitive emperor asked why he could not find God in Laplace's work. The response from Laplace to the emperor was "*je n'ai pas besoin de cette hypothèse*" which translates to "I have no need for this hypothesis". In light of this, the criteria for constructing models relies on simplicity combined with accuracy with respect to empirical evidence.

Provided this standard, there are two ways of constructing mechanistic models. Either the construction procedure starts from a large⁵ initial model which subsequently is reduced or it starts from a small simple model which then is expanded. In this thesis, it is the latter approach that has been implemented to construct the presented models. By the terms "simple" and "complex" model structures, one refers to the mathematical properties of the reaction terms⁶. Specifically, a simple model consists of linear reaction terms while a slightly more complex structure involves polynomial non-linearities and lastly an even more complex structure involves the quotient based non-linearities found in enzyme kinetics (e.g. (2.4) on page 21). Although this statistical criteria for model selection provides a "rule of thumb" when constructing mechanistic models, it is often not sufficient in order to conclusively find the correct underlying mechanism as there are generally multiple plausible models of the system at hand. In particular, this has been evident in both the case of the models describing the replicative life span of yeast on a large time scale (Chapter 3) as well as in the case of the models of Cdc42-mediated cell polarisation on a small time scale (Chapter 4). The first step in finding a methodology for constructing models in an unambiguous and non-arbitrary fashion is to identify reasons for why it is often the case that numerous different models cannot be distinguished.

One potential cause of the described problem is the fundamental assumption of the statistical methodology. It is namely the case that multiple statistical criteria originate from the field of parameter estimation which entails estimating the kinetic parameters in a given model that best replicate the data. However, the key assumption of parameter estimation is given that *the presented model is true* one wishes to find the parameters that minimise the distance between the simulated and measured outputs. Moreover, as this typically implies solving an ill-posed optimisation problem⁷ there are often numerous kinetic parameters that can replicate the data independent of the model structure.

⁵A "large" model usually refers to the number of states.

⁶The reaction terms are determined by the functions f and g respectively in (2.5) and (2.6) on page 22.

⁷More specifically, the optimisation problem is commonly expressed as in (2.16) or (2.17) on page 32. By ill-posed we mean that the problem has multiple local optima whereas well-posed means that the problem has one unique solution.

Thus, the parameter estimation approach is more interested in using the model as a tool for connecting inputs to outputs (Fig 1.1) as oppose to finding the adequate model structure for the system of interest. To illustrate the problem occurring in the context of statistically based model selection, consider the analogy of the “blind men and the elephant” (Fig 5.1) [40]. Imagine that two blind men touch the trunk of an elephant where one of them correctly assumes that he touches a trunk and the other assumes that he touches a snake. Then given the observed output, that is the touch of the trunk, it is impossible to differentiate between the two models, that is the elephant trunk versus the snake. However, the actual description of the model is essential in order to draw correct conclusions about the system at hand. This is exactly the nature of the presented problem and as mechanistic modellers we are all blind men describing a complex system. The inability to deduce the correct mechanism decreases the reliability of the predictions of the models and it limits the capacity to extrapolate from the model in order to discover unknown properties of the system at hand. Therefore, it is highly desirable to find a more rigorous methodology for constructing mechanistic models.

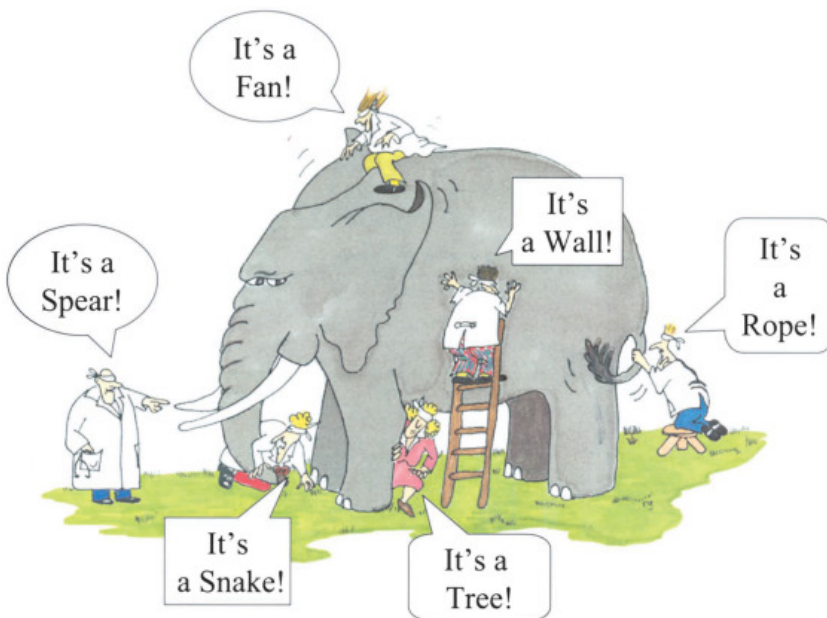


Figure 5.1: The blind men and the elephant. The cartoon initially presented in [40] was drawn by Renee Guzlas. The authors of the article Jonathan Himmelfarb, Alp Ikizler and Hakim Raymond as well as the sister of the artist Rebecca Wingard have personally granted me permission to use the figure through e-mail correspondence.

Ideally, the construction of models would be based on estimating structures from measured data. Thus, instead of assuming that the model is true in order to estimate its kinetic parameters which is classically done in model selection, the underlying assumption would be to find structures in the data which subsequently are used to construct models. If this is possible, this would not only render the procedure for constructing models more rigorous it would also increase the reliability of the models and increase the likelihood of finding the true mechanism of the system of interest. Nonetheless, these structures that are to be found in the data must be encoded mathematically in order to be able to formalise such a framework for constructing mechanistic models. In my experience, this can be achieved by a specific mathematical tool called *symmetry methods*, see subsection 2.2.6. Symmetries are particular mathematical objects⁸ which capture the “physical laws” that a system obeys such as energy and mass conservation or rotational invariance. This type of mathematical tool has been used with enormous success in fundamental physics where a specific example of the usage of symmetry methods is the standard model of elementary particle physics [113, 120]. In mathematical biology, these methods are much more uncommon (see [33] for examples) and currently the focus is on finding analytical solutions to models in order to analyse their mathematical properties. Nonetheless, in analogy with the problem of statistical model selection, it is mainly interesting to analyse the mathematical properties of a mechanistic model if the model actually is true in some sense. To this end, the idea is to use these methods to construct mechanistic models that satisfy various physical properties concealed in experimental data which can be revealed by the symmetries.

In Paper V, we showcase the power of symmetry methods in addressing a minimal problem of model selection in the context of enzyme kinetics. Particularly, we propose a symmetry based framework for selecting different candidate models that fit (in the least square sense) time series data approximately equally well. The major conclusion from Paper V is that when the statistically based methodology for model selection is inconclusive, symmetries can in fact find the underlying mechanism of a system and also reject faulty model structures. These results indicate that symmetries can reveal the properties that govern a system which can subsequently be used to construct reliable models. Further, this will increase the reliability of the predictions made by specific models which has a huge potential in the context of mechanistic modelling.

The vision of implementing symmetries in mechanistic modelling is to increase the validity of the models. By estimating the symmetries that govern a system

⁸Symmetries are operators that preserve structure. In the context of differential equations, symmetries map solutions to other solutions (see section 2.2.6 on page 36).

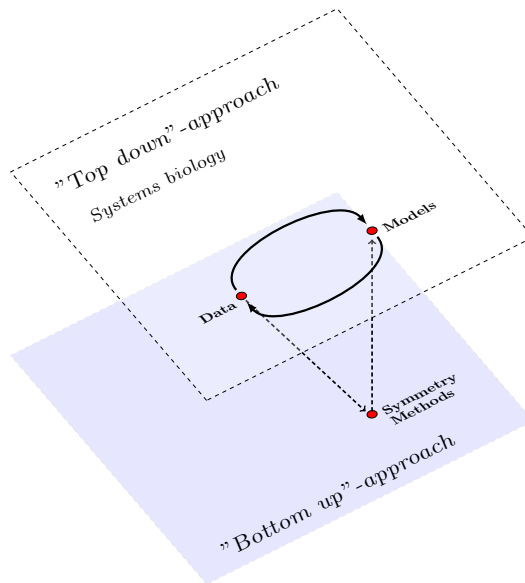


Figure 5.2: The vision of symmetries in mechanistic modelling.

from experimental data, it is possible to construct models *directly*⁹ from the symmetries. This theoretical "bottom-up" approach will sidestep the current ambiguity associated with the construction of models and most importantly it will increase the validity of the structure of the model at hand. In turn, this will increase the accuracy of the predictions and this framework can naturally be coupled to the currently well-known *systems biology cycle* [56, 57]. The workflow of this "top down" approach consists of constructing models which are calibrated by experimental data, then novel experiments are conducted which are subsequently used to modify the models and this is repeated in a cyclic fashion. The coupling of these two approaches (Fig 5.2) entailing the introduction of symmetries into mechanistic modelling will greatly enhance the impact of mathematical models in biology. This is due to the fact that, in this scenario, the underlying physical properties of biological systems can be captured by the models, allowed by the use of symmetries, in a manner that currently is not possible.

In this way, the models will not only be more realistic than they currently are,

⁹*Variational symmetries* occur in variational problems which entail the maximisation or minimisation of a functional with a corresponding integrand called the Lagrangian [45, 79]. In this context, an ODE, i.e. a model, can be derived directly from a variational principle [45, 79].

but they will also encode information about the system that is not accessible by standard means. Consequently, the construction and analysis of models will not only be a matter of engaging in an interesting mathematical exercise, but the models will be essential in revealing fundamental properties of biological systems similar to the role that modelling plays in physics. Thus, the focus of mathematical modelling in biology will be switched from merely reproducing experimental data to actually analysing the structure of the models in order to capture the underlying mechanisms. Thereby, the understanding of the system of interest will increase which, in turn, will greatly enhance the relevance of models in numerous applications. Finally, given a correct mechanistic model, a single simulation corresponds to an actual experiment which (in times of immense computational capabilities) will vastly increase the capacity to understand diseases and potentially finding cures to illnesses.

6 Summary of papers

6.1 Paper I - Systems Biology of Ageing

The ambition of the work was to showcase how the integration of data into modelling can lead to novel insights about the ageing phenomena. In this book chapter, an overview of both the mathematical models used in research related to ageing and the relevant biology including numerous evolutionary theories are described. Furthermore, four small kinetic models of damage accumulation corresponding to distinct ageing strategies were proposed corresponding to different means of ageing that an individual cell can undergo. In particular, these strategies were defined by two traits, namely by cells having or lacking a capacity to repair damage and by cells which could retain or not retain damage. Based on these strategies, we speculated that the environment of the cell determines which strategy that is beneficial and based on this we suggested that cells could principally switch between different strategies determined by the environmental conditions so as to increase the growth rate or improve the overall fitness of the population.

6.2 Paper II - Synergistic effects of repair, resilience and retention of damage determine the conditions for replicative ageing

The purpose was to build a model of replicative ageing focusing on the major factors involved in the accumulation of damaged proteins in the budding yeast *S. cerevisiae*. To this end, a comprehensive single cell description, based on ODEs, of the accumulation of damaged proteins involving the forces cell growth, formation and repair of damage was constructed. Additionally, the cell

division entailing the generation of two cells from one and the inheritance of damage was described by a discrete part which was coupled to the continuous part corresponding to the formation of damage due to cell growth. Importantly, we introduced a threshold value on the accumulated damage determining when cell death occurs, and this enabled us to investigate the effect of altering individual parameters on the replicative life span of individual cells. Using non-dimensionalisation, we introduced the key property of *resilience to damage* that could empirically be measured by the increase in volume of an individual cell over the course of its life-span. Using experimental data consisting of growth curves we could not only validate the model but also show that it outperforms other candidate models. Also, using mathematical analysis of the properties of the model, we could derive two theoretical upper bounds on the degree of asymmetry in the cell division as well as the maximum amount of damage a mother cell can retain. Lastly, using simulations we were able to compare different strategies for prolonging the life span of individual cells such as reducing the formation of damage or increasing the capacity to repair damage as well as comparing the effect of dividing symmetrically, e.g. the bacteria *E.coli*, with dividing asymmetrically, e.g. the budding yeast *S. cerevisiae*.

6.3 Paper III - Selective benefits of producing daughter cells of unequal reproductive potential in the population of a unicellular organism

Building from the model in Paper II, we expanded the focus to include how factors on the single cell level affect an entire population of cells. To this end, we firstly took the individuality of the single cells into account by introducing non-linear mixed effects in the rate parameters corresponding to the rate of repair and rate of damage formation. Also, a novel more realistic repair profile, which declines with high age and that corresponds to an efficient repair machinery early in life, was introduced. By simulating the growth of the population as well as monitoring all the various lineages of cells, a computational framework for investigating the well-being of the entire population was introduced. The quantitative measures of this well-being included known metrics such as average generation time, growth rate, distribution of damage throughout the population, the replicative life span and population size but we also introduced a novel metric called the *health span*. The latter property corresponds to the proportion of the life time of an individual cell which it spent as "healthy" meaning that it had less damage than a specified threshold value. Using large scale simulations, we determined that the novel repair

profile resulted in shorter generation times and longer health spans compared to a constant repair profile. Furthermore, we saw that populations of mother cells with retention had less variability in terms of the replicative life span and the health span compared to populations without. Finally, this difference in variability could be traced back through the lineages where this finding was explained by the fact that in populations with retention the mother cells are more similar to their daughters compared to populations without retention.

6.4 Paper IV - Cell polarisation in a bulk-surface model can be driven by both classic and non-classic Turing instability

In this paper, we focus our attention on the details of the cell polarisation by modelling the dynamics of the protein Cdc42. More precisely, Cdc42 is shuffled between its active and inactive state in the membrane where the active state aggregates at a specific spatial location called the pole where the budding occurs. There is also a transport of inactive Cdc42 from the cytosol, i.e. from within the cell, to the membrane and thus accounting for both the cytosol and the membrane in the spatial description of the model is crucial. However, this is something that numerous previous models of Cdc42 have neglected where they solely focus on the aggregation of active Cdc42 in the membrane (i.e. a two dimensional domain) which is achieved by the mathematical phenomena diffusion driven instability. To this end, we constructed a so called bulk-surface model entailing a three dimensional description of the cell including both the cytosol and the membrane. Further, we proved the existence of a unique solution to the proposed RD model in global time as well as that the proposed model can undergo diffusion driven instability through both classic and so called non-classic Turing instability. Also, a thorough numerical investigation of the parameter space was conducted in order to elucidate the parameters that allow for pattern formation in the concentration profile which, in this context, entails the formation of a single pole of active Cdc42 in the membrane. From the mapping of the parameter space, we were able to relate the classic case of Turing instability, which requires that the active form diffuses slower than the inactive form corresponding to a relative diffusion of $d > 1$, to the more recent non-classic case in which both forms can diffuse with the same rate, e.g. $d = 1$. In fact, we proposed that the non-classic case corresponds to the classic counterpart in the limit $d \rightarrow 1$. Subsequently, we validated these theoretical results by means of simulations where we showed that the model can simulate cell polarisation. Lastly, we conducted quantitative simulations (which is rare

for PDE models which require substantial computational power) in order to investigate the effect of changing kinetic parameters and the size of the cell on measurable outcomes such as the size of the pole, the time to polarisation and the number of poles formed.

6.5 Paper V - Symmetry structures in dynamic models of biochemical systems.

The intention of this paper was to provide a minimal example of how symmetries relate to the structure of ODE models in systems biology. To this end, we studied a simple chemical reaction where a substrate is converted to a product catalysed by an enzyme, and specifically merely one time-series of substrate concentration was available. Moreover, three candidate models based on the famous Hill-Langmuir equation corresponding to one, two and three active sites respectively were fitted to a time-series where one of the three candidate models was used to generate the data, i.e. was the correct one. Then, in a situation where the experimental noise was large relative to the intrinsic noise between different models, regular model fitting in terms of the “least-squares” could not distinguish between the various candidates. To achieve this task, we proposed a symmetry based methodology for selecting the correct model where the starting point was that symmetries that were *unique* to each candidate model were derived. Then, the methodology proceeded in four steps: (1) transform the time-series using the symmetry, (2) fit in the sense of “least squares” the candidate to the model to the transformed time series, (3) transformed the fitted model “back” using the inverse transform and (4) compare the inversely transformed model to the original time series. If the candidate model generated the data it should be invariant under the action of the symmetry, while in the case that the candidate model did not underlie the data the corresponding transformation would have distorted the time series and thereby reduced the fit. Lastly, we showed that that our symmetry based methodology outperforms the classic “least square” methodology as the correct model was selected in all investigated cases. This demonstrates that symmetries can reveal “hidden” structures that cannot be detected using statistical methods in situations where data is scarce and the experimental error is large enough.

7 Conclusions and outlook

The progress of the increasingly interdisciplinary life sciences relies on bridging the gap between the simplicity of models and the complexity of biology. From a mathematical point of view, the sentiment that “models should be as simple as possible” has its merit. On the one hand, this principle results in models without superfluous details, captured by the term *identifiability* (see subsection 2.2.5 and 2.2.7), which enables researchers to distil the important components of a studied system. On the other hand, it renders the models manageable in the sense that they can be analysed which, in the best case scenario, reveals fundamental properties of, for example, a studied protein being integral to the progress of a particular disease. However, from the experimental point of view, the objection to this perspective is that the complexity of biology is *vast* and the simplicity of numerous models results in theoretical descriptions that have no or little bearing on reality.

One answer to this objection by the theoreticians, which obstructs interdisciplinarity, is to ignore it. This entails that models of biological systems are constructed for the sake of modelling due to, for instance, an interest in their exciting mathematical properties where the validity of the models in terms of biology is neglected or not prioritised. A concrete example reflecting this mentality is the vast number of mathematical models produced of the activity of Cdc42 [15, 20, 21, 32, 34, 35, 49, 50, 61, 71, 81, 95, 107, 109] largely driven by the captivating mathematical phenomena called Turing instability where the biological relevance of the models arguably is not the focus. Personally, I think the objection by the experimentalists is completely valid and that theoreticians should focus on the relevance of their models. However, the response by the experimentalists in turn should not be the literal opposite of the simplicity based value of mechanistic modelling, namely that “(biological) models should be as complex as possible”. In my opinion, it is a version, perhaps not as vulgarly put, of the latter statement that is the cause of another worrying trend in the field of systems biology in particular.

Alternatively, the answer to biological complexity is complexity in the models. Accordingly, in order to capture as much details of a biological system as possible, the answer from a modelling point of view is to construct very large models in terms of the number of states and parameters. An objection from the modellers to this approach relates to issues of identifiability, where models including too many, i.e. in the range 10-100, kinetic parameters will, in practice, be impossible to identify. Another one, is that these extensive models are virtually impossible to analyse and validate which implies that the power of mathematical modelling entailing the capacity to propose novel mechanisms as well as making predictions of unknown outcomes is lost. One answer to this objection by the experimentalists, which again obstructs interdisciplinarity, is to ignore these objections and only focus on the capacity of the models to reproduce data. The expression of this trend is exemplified by numerous works in which large models of, for example, intracellular signalling pathways of proteins are merely evaluated based on their capacity to reproduce data but where properties of the models such as stability or identifiability is wholly neglected. This is somewhat in the vein of statistical modelling (Fig 1.1 on page 2) where models are viewed as a tool for connecting some (explanatory) variables or inputs to an observed output, as oppose to a theoretical framework for understanding the underlying mechanisms of a biological system. Moreover, a problem with this approach is that the explanatory capacity of these models are often restricted to the data they are validated by and thus they cannot be used in order to explain other properties, than the experimentally observed ones, of the system of interest. Also, it is often not possible to differentiate between candidate models, especially not if the models have too many states and parameters, and thus it is not possible in this case to deduce fundamental properties of the studied system.

I think the future of mechanistic modelling should take a golden middle way between these two perspectives. On the one hand, the theoretical models should be better motivated by biological knowledge, more focused on explaining experimental data and they should ultimately involve more detail, i.e. become larger. On the other hand, the structure and the mathematical properties of the models should be analysed as this can elucidate the underlying mechanisms of the studied biological system. In relation to experimental data, the focus should be to extract structural information used to construct models and not only to use the models in order to reproduce an observed output. Thus, the focus should not necessarily be to generate more, in terms of quantity, data but to develop methodologies enabling the extraction of more *information* in the data which can be used to validate the structure of the models. I believe that a part of the answer to both of these challenges can be provided by symmetry methods (see subsection 2.2.6 and Paper V). When it comes to the first challenge of constructing more biologically relevant models as well as increasing

their size, the starting point could be to deduce which physical properties that biological systems obey and how to encode these in symmetries. Then, models could be derived directly from these symmetries and also, in contrary to model reduction, a framework for scaling up models could be implemented based on the properties encoded in symmetries. Regarding the second challenge of extracting structural information from empirical data, a procedure of “*model structure estimation*” similar to that of parameter estimation (see subsection 2.2.5) could be implemented based on symmetries. This would preferably be formulated as an optimisation problem where the optimal solution corresponds to the symmetries that describe patterns or structures in the data. Given these symmetries, it would then be possible to derive an appropriate model of the studied system. Currently, numerical approaches for finding model structures in dynamical modelling [104] including reaction diffusion models in the context of Turing instability [98] are based on machine learning where a script (blindly) evaluates, through simulations, numerous different candidate models. Despite the capacity of modern high performance computing platforms, the set of possible model structures is, most likely, so enormous that the probability of finding a “true” model structure by, essentially, guessing is stupendously low. In the context of parameter estimation, this would be consistent with an algorithm that generates different parameter guesses in order to calibrate a model and then the corresponding optimal set of parameters that is saved would be the guess resulting in the best fit.

The key to accomplish this task is to automate the above procedure. The symmetry based framework for both extracting information about model structures from experimental data as well as analysing large models using symmetries rely on the development of efficient computer based algorithms. A source of inspiration in this respect could be the software developed by Karlsson et al. [53] which conducts a structural identifiability analysis (see subsection 2.2.7) of a provided dynamic model using symbolic calculations. In conclusion, novel theoretical tools for constructing, validating and analysing mathematical models in biology must be implemented in order to cope with complexity as well as obtaining a deeper understanding of the inner workings of living organisms.

8 Glossary of fundamental biological terms

Here follows, in my opinion, the fundamental terms necessary for understanding the biological aspects of the thesis. For further reading, the book entitled “Molecular Biology of The Cell” by Alberts et al. [2] is recommended and it is this source that the descriptions of the terms below are based on.

Polymer

A large molecule which links numerous smaller identical units, called monomers, together. The monomers are connected through so called “covalent bonds” which are a strong type of chemical bond. Two important classes of polymers are the *polynucleotides*, e.g. *DNA* and *RNA*, and the *proteins*.

Monomer

A small molecules which constitutes the building blocks or subunits of larger molecules called polymers.

DNA

Deoxyribonucleic acid (DNA) is a polymer where the monomers are called *deoxyribonucleotides*. The monomers consist of three components: a nitrogen base, a sugar molecule and phosphate groups. The nitrogen bases are further divided into two classes, purines and pyrimidines. The purines are called *adenine* (A) and *guanine* (G) while the pyrimidines of DNA are called *cytosine* (C) and

thymine (T). The sugar molecule in DNA is called *deoxyribose* and together with the phosphate group it can bind covalently to other nucleotides forming what is referred to as the “backbone” of the DNA molecule. On the backbone, there are numerous bases attached and together with the backbone they form a strand of DNA. Moreover, the nitrogen bases can bind to other bases through hydrogen bonds enabling the connection of two different strands of DNA, and such DNA molecules are referred to as *double stranded*. Regarding the binding of the nitrogen bases, the purines can bind to the pyrimidines according to the following rules: A binds to T and G bind to C. Also, a list of the hydrogen bases on a strand, e.g. “ATGTCCTAGAC”, is called a DNA sequence and it is in the form of these sequences that the information about all essential functions of the cell is encoded. Another key property of DNA is that the chemical bonds between the bases of two different strands are weaker than the bonds between the phosphate groups and the sugar molecules in the backbone. Consequently, it is possible to separate strands of DNA without breaking the backbone and the chemical properties of this polymer also determine its physical configuration.

The three dimensional shape of the DNA molecule is a consequence of its electrochemical properties. The interior of the cell is mostly filled with water, H_2O , which is a so called *dipolar* molecule. Although this type of compound has no net charge if one take the whole molecule into account, more electrons, in the case of water, are located by the oxygen atom resulting in a partial negative charge while the hydrogen atoms yield a partial positive charge. In addition, a fundamental property of chemistry is that charged molecules are often called “hydrophilic” as they can interact with water while uncharged molecules that avoid water are called “hydrophobic” implying that they do not react with water. In the context of DNA, the hydrogen bases are hydrophobic and the backbone is hydrophilic due to the phosphate group. A striking fact about the phosphate groups is that they are very negatively charged which is used in experimental techniques when, for example, the sizes of a DNA fragments are measured¹. Moreover, the negative charge of the backbone results in the fact that it is often, in a charged media such as water, faced outwards towards the media while the uncharged and flat nitrogen bases are faced inwards. Due to this difference in electrical charge, the well-known structure of the DNA in many eukaryotes is called the *double helix*, initially proposed by Watson and Crick [112]. There are also other shapes that DNA polymers can take on, and one of them is the circular shape of a plasmid (see subsection 2.1.4 on page 14) found in, among other organisms, bacteria.

¹For instance, in the case of an *agarose gel* sugar molecules form a network structure in which one can insert DNA fragments. If an electrical current is applied over the gel, the DNA molecules will move towards the positive node and larger molecules will move slower through the gel which enables researchers to measure the size of the DNA molecules.

RNA

Ribonucleic acid (RNA) is a polymer where the monomers are called *Ribonucleotides* and it differs from DNA in three respects. Firstly, the sugar molecule in RNA is called *ribose* as oppose to deoxyribose in DNA. Secondly, RNA has a nitrogen base called *uracil (U)* which replaces the thymine (T) in DNA. Thirdly, RNA molecules can be single stranded unlike DNA molecules (at least most of the time). There are three important types of RNA called *messenger RNA (mRNA)*, *transfer RNA (tRNA)* and *ribosomal RNA (rRNA)*. The mRNA's convey the information encoded in the DNA, the tRNA's act as an interface between the mRNA and the particle called the ribosome (read more under "translation" below) and the rRNA's are constituents of the ribosomes.

Proteins

Proteins are polymers where the monomers are called *amino acids*. There are 21 amino acids which render them more numerous than the four types of monomers defining the polynucleotides. Furthermore, each amino acid has different chemical properties such as electrical charge which, in turn, implies that the overall structure of a protein as well as its reactivity in terms of binding to other molecules are largely determined by the amino acids that make up the specific protein of interest. Also, the amino acids are linked together by so called *peptide bonds* in order to form a sequence which identifies the protein in question. Due to these bonds, they are also referred to as *polypeptides* and they do not only constitute the building blocks of the cell but they also execute the majority of its functions. As previously mentioned, an important aspect of the protein is its three dimensional shape which is determined by the sequence of amino acids due to the different chemical properties of each amino acid. If a protein loses its shape, it also loses its function and an accumulation of this type of "damaged" proteins is often a symptom of ageing in numerous organisms. A particularly important class of proteins are the enzymes.

The central dogma of molecular biology

The process by which the information encoded in DNA gets executed by proteins is called the *central dogma of molecular biology*. It is central to all forms of life and includes three major steps: the replication, the transcription and the translation. The flow of information from DNA to proteins goes through an intermediary step using RNA.

Replication

The *replication* is the process resulting in the copying or duplication of DNA. The particular protein which aids this process is called *DNA polymerase* which synthesises a new DNA molecule by joining together nucleotides based on the information encoded in an existing DNA polymer which is used as a template.

Transcription

The *transcription* of a DNA strand is the creation of a complementary RNA sequence. This process is aided by a protein called *RNA polymerase* which joins ribonucleotides together in order to form a RNA polymer by using DNA as a template.

Translation

The *translation* of a mRNA sequence entails the construction of a protein. This is achieved after numerous amino acids have been joined together which is a process that occurs on the ribosomes. The ribosomes are particles made of various proteins and rRNAs which catalyse the synthesis of proteins from mRNA.

Gene

A *gene* is a sequence of DNA which is transcribed as a single unit to either a single protein or a single RNA molecule. Thus, it is the genes that contain the hereditary information encoded in DNA. In other words, a gene corresponds to a piece of “code” corresponding to a single or several functions in the cell.

Enzyme

An *enzyme* is a protein which acts as a *catalyst* of specific chemical reactions. In other words, it takes part in the reaction by increasing the reaction rate without being consumed itself. The molecule which an enzyme acts on is called the *substrate* which is subsequently converted into another molecule called the *product* of the enzyme. The substrate binds in to a specific part of the enzyme called the *active site* where the reaction occurs. From the point of view of nomenclature, the names of most enzymes end with the suffix “-ase” and

examples are the polymerases involved in the replication and transcription described above.

Bibliography

- [1] H. Aguilaniu, L. Gustafsson, M. Rigoulet, and T. Nyström. Asymmetric inheritance of oxidatively damaged proteins during cytokinesis. *Science*, 2003.
- [2] B. Alberts, A. Johnson, J. Lewis, M. Raff, K. Roberts, and P. Walter. *Molecular Biology of the Cell*. Garland Science, Taylor & Francis Group, New York, 5 ed. edition, 2008.
- [3] N. Andreasson, A. Evgrafov, and M. Patriksson. *An introduction to continuous optimization: foundations and fundamental algorithms*. Courier Dover Publications, 2020.
- [4] M. Anguelova. *Observability and identifiability of nonlinear systems with applications in biology*. Chalmers University of Technology Gothenburg, Sweden, 2007.
- [5] P. Atkins and L. Jones. *Chemical principles: The quest for insight*. Macmillan, 2007.
- [6] C. T. H. Baker, G. A. Bocharov, J. M. Ford, P. M. Lumb, S. J. Norton, C. A. H. Paul, T. Junt, P. Krebs, and B. Ludewig. Computational approaches to parameter estimation and model selection in immunology. *Journal of Computational and Applied Mathematics*, 184(1):50–76, 2005.
- [7] A. A. Barton. Some aspects of cell division in *Saccharomyces cerevisiae*. *Microbiology*, 4(1):84–86, 1950.
- [8] P. Bharadwaj, R. Martins, and I. Macreadie. Yeast as a model for studying Alzheimer’s disease. *FEMS Yeast Research*, 10(8):961–969, 2010.
- [9] E. Bi and H.-O. Park. Cell polarization and cytokinesis in budding yeast. *Genetics*, 191(2):347–387, 2012.

- [10] R. A. Bradshaw and E. A. Dennis. *Handbook of cell signaling*. Academic press, 2009.
- [11] G. Cedersund and J. Roll. Systems biology: model based evaluation and comparison of potential explanations for given biological data. *The FEBS journal*, 276(4):903–922, 2009.
- [12] W. Chen, H. H. Lim, and L. Lim. The CDC42 homologue from *Caenorhabditis elegans*. Complementation of yeast mutation. *Journal of Biological Chemistry*, 268(18):13280–13285, 1993.
- [13] E. W. Cheney and D. R. Kincaid. *Numerical mathematics and computing*. Cengage Learning, 2012.
- [14] J.-g. Chiou, M. K. Balasubramanian, and D. J. Lew. Cell Polarity in Yeast. *Annual Review of Cell and Developmental Biology*, 2017.
- [15] J.-G. Chiou, S. A. Ramirez, T. C. Elston, T. P. Witelski, D. G. Schaeffer, and D. J. Lew. Principles that govern competition or co-existence in Rho-GTPase driven polarization. *PLoS computational biology*, 14(4):e1006095, 2018.
- [16] R. J. Clegg, R. J. Dyson, and J.-U. Kreft. Repair rather than segregation of damage is the optimal unicellular aging strategy. *BMC biology*, 12(1):1, 2014.
- [17] D. Cusseddu, L. Edelstein-Keshet, J. A. Mackenzie, S. Portet, and A. Madzvamuse. A coupled bulk-surface model for cell polarisation. *Journal of theoretical biology*, 2018.
- [18] L. Debnath, P. Mikusinski, and Others. *Introduction to Hilbert spaces with applications*. Academic press, 2005.
- [19] J. DiStefano III. *Dynamic systems biology modeling and simulation*. Academic Press, 2015.
- [20] B. Drawert, S. Hellander, M. Trogdon, T.-M. Yi, and L. Petzold. A framework for discrete stochastic simulation on 3D moving boundary domains. *The Journal of Chemical Physics*, 145(18):184113, 2016.
- [21] J. M. Dyer, N. S. Savage, M. Jin, T. R. Zyla, T. C. Elston, and D. J. Lew. Tracking shallow chemical gradients by actin-driven wandering of the polarization site. *Current biology*, 23(1):32–41, 2013.
- [22] S. Eaton, P. Auvinen, L. Luo, Y. N. Jan, and K. Simons. CDC42 and Rac1 control different actin-dependent processes in the *Drosophila* wing disc epithelium. *The Journal of cell biology*, 131(1):151–164, 1995.

- [23] L. Edelstein-Keshet. *Mathematical models in biology*. SIAM, 2005.
- [24] E. Eriksson, K. Sott, F. Lundqvist, M. Sveningsson, J. Scrimgeour, D. Hanstorp, M. Goksör, and A. Granéli. A microfluidic device for reversible environmental changes around single cells using optical tweezers for cell selection and positioning. *Lab on a Chip*, 10(5):617–625, 2010.
- [25] N. Erjavec, M. Cvijovic, E. Klipp, and T. Nyström. Selective benefits of damage partitioning in unicellular systems and its effects on aging. *Proceedings of the National Academy of Sciences of the United States of America*, 2008.
- [26] N. Erjavec, L. Larsson, J. Grantham, and T. Nyström. Accelerated aging and failure to segregate damaged proteins in Sir2 mutants can be suppressed by overproducing the protein aggregation-remodeling factor Hsp104p. *Genes and Development*, 2007.
- [27] N. Erjavec and T. Nyström. Sir2p-dependent protein segregation gives rise to a superior reactive oxygen species management in the progeny of *Saccharomyces cerevisiae*. *Proceedings of the National Academy of Sciences of the United States of America*, 2007.
- [28] M. C. Florian, K. Dörr, A. Niebel, D. Daria, H. Schrenzenmeier, M. Rojewski, M.-D. Filippi, A. Hasenberg, M. Gunzer, K. Scharffetter-Kochanek, and Others. Cdc42 activity regulates hematopoietic stem cell aging and rejuvenation. *Cell stem cell*, 10(5):520–530, 2012.
- [29] K. Gardner, P. A. Hall, P. F. Chinnery, and B. A. I. Payne. HIV treatment and associated mitochondrial pathology: review of 25 years of in vitro, animal, and human studies. *Toxicologic pathology*, 42(5):811–822, 2014.
- [30] H. Geiger and Y. Zheng. Cdc42 and aging of hematopoietic stem cells. *Current opinion in hematology*, 20(4):295, 2013.
- [31] L. Geris, D. Gomez-Cabrero, and Others. *Uncertainty in biology*. Springer, 2016.
- [32] W. Giese, M. Eigel, S. Westerheide, C. Engwer, and E. Klipp. Influence of cell shape, inhomogeneities and diffusion barriers in cell polarization models. *Physical biology*, 12(6):66014, 2015.
- [33] M. Golubitsky and I. Stewart. Symmetry methods in mathematical biology. *São Paulo Journal of Mathematical Sciences*, 9:1–36, 2015.
- [34] A. B. Goryachev and M. Leda. Many roads to symmetry breaking: molecular mechanisms and theoretical models of yeast cell polarity. *Molecular biology of the cell*, 28(3):370–380, 2017.

- [35] A. B. Goryachev and A. V. Pokhilko. Dynamics of Cdc42 network embodies a Turing-type mechanism of yeast cell polarity. *FEBS letters*, 582(10):1437–1443, 2008.
- [36] L. Guarente. Mitochondria-A Nexus for Aging, Calorie Restriction, and Sirtuins?, 2008.
- [37] D. Harman. The Biologic Clock: The Mitochondria? *Journal of the American Geriatrics Society*, 1972.
- [38] S. M. Hill, S. Hanzén, and T. Nyström. Restricted access: spatial sequestration of damaged proteins during stress and aging. *EMBO reports*, 18(3):377–391, 2017.
- [39] S. M. Hill, X. Hao, J. Grönvall, S. Spikings-Nordby, P. O. Widlund, T. Amen, A. Jörhov, R. Josefson, D. Kaganovich, B. Liu, and Others. Asymmetric inheritance of aggregated proteins and age reset in yeast are regulated by Vac17-dependent vacuolar functions. *Cell reports*, 16(3):826–838, 2016.
- [40] J. Himmelfarb, P. Stenvinkel, T. A. Ikizler, and R. M. Hakim. The elephant in uremia: oxidant stress as a unifying concept of cardiovascular disease in uremia. *Kidney international*, 62(5):1524–1538, 2002.
- [41] C. Hitchens. *God is not great: How religion poisons everything*. McClelland & Stewart, 2008.
- [42] K. Holmåker and I. Gustafsson. *Linjär algebra : fortsättningskurs*. Liber, 2016.
- [43] L. Hörmander. *The analysis of linear partial differential operators I: Distribution theory and Fourier analysis*. Springer, 2015.
- [44] S. Hug, D. Schmidl, W. B. Li, M. B. Greiter, and F. J. Theis. Bayesian model selection methods and their application to biological ODE systems. In *Uncertainty in Biology*, pages 243–268. Springer, 2016.
- [45] P. E. Hydon. *Symmetry methods for differential equations: a beginner's guide*, volume 22. Cambridge University Press, 2000.
- [46] A. Iserles. *A first course in the numerical analysis of differential equations*. Number 44. Cambridge university press, 2009.
- [47] J. Y. Jang, A. Blum, J. Liu, and T. Finkel. The role of mitochondria in aging. *The Journal of clinical investigation*, 128(9):3662–3670, 2018.
- [48] S. M. Jazwinski, N. K. Egilmez, and J. B. Chen. Replication control and cellular life span. *Experimental gerontology*, 24(5):423–436, 1989.

- [49] A. Jilkine and L. Edelstein-Keshet. A comparison of mathematical models for polarization of single eukaryotic cells in response to guided cues. *PLoS computational biology*, 7(4):e1001121, 2011.
- [50] A. Jilkine, A. F. M. Marée, and L. Edelstein-Keshet. Mathematical model for spatial segregation of the Rho-family GTPases based on inhibitory crosstalk. *Bulletin of mathematical biology*, 69(6):1943–1978, 2007.
- [51] D. I. Johnson and J. R. Pringle. Molecular characterization of CDC42, a *Saccharomyces cerevisiae* gene involved in the development of cell polarity. *The Journal of cell biology*, 111(1):143–152, 1990.
- [52] R. Josefson, R. Andersson, and T. Nyström. How and why do toxic conformers of aberrant proteins accumulate during ageing? *Essays in biochemistry*, 61(3):317–324, 2017.
- [53] J. Karlsson, M. Anguelova, and M. Jirstrand. An efficient method for structural identifiability analysis of large dynamic systems. *IFAC proceedings volumes*, 45(16):941–946, 2012.
- [54] J. Kim. Validation and selection of ODE models for gene regulatory networks. *Chemometrics and Intelligent Laboratory Systems*, 157:104–110, 2016.
- [55] T. B. Kirkwood. Evolution of ageing. *Nature*, 270(5635):301–304, 1977.
- [56] H. Kitano. Perspectives on systems biology. *New Generation Computing*, 18(3):199–216, 2000.
- [57] H. Kitano. Computational systems biology. *Nature*, 420(6912):206–210, 2002.
- [58] E. Klipp, W. Liebermeister, C. Wierling, and A. Kowald. *Systems biology: a textbook*. John Wiley & Sons, 2016.
- [59] S. Larsson and V. Thomée. *Partial differential equations with numerical methods*, volume 45. Springer Science & Business Media, 2008.
- [60] P. Laun, A. Pichova, F. Madeo, J. Fuchs, A. Ellinger, S. Kohlwein, I. Dawes, K. U. Fröhlich, and M. Breitenbach. Aged mother cells of *Saccharomyces cerevisiae* show markers of oxidative stress and apoptosis. *Molecular Microbiology*, 2001.
- [61] A. T. Layton, N. S. Savage, A. S. Howell, S. Y. Carroll, D. G. Drubin, and D. J. Lew. Modeling vesicle traffic reveals unexpected consequences for Cdc42p-mediated polarity establishment. *Current Biology*, 21(3):184–194, 2011.

- [62] J. Liepe, P. Kirk, S. Filippi, T. Toni, C. P. Barnes, and M. P. H. Stumpf. A framework for parameter estimation and model selection from experimental data in systems biology using approximate Bayesian computation. *Nature protocols*, 9(2):439, 2014.
- [63] S. J. Lin, M. Kaeberlein, A. A. Andalis, L. A. Sturtz, P. A. Defossez, V. C. Culotta, G. R. Fink, and L. Guarente. Calorie restriction extends *saccharomyces cerevisiae* lifespan by increasing respiration. *Nature*, 2002.
- [64] B. Liu, L. Larsson, A. Caballero, X. Hao, D. Öling, J. Grantham, and T. Nyström. The Polarisome Is Required for Segregation and Retrograde Transport of Protein Aggregates. *Cell*, 2010.
- [65] B. Liu, L. Larsson, V. Franssens, X. Hao, S. M. Hill, V. Andersson, D. Höglund, J. Song, X. Yang, D. Öling, J. Grantham, J. Winderickx, and T. Nyström. Segregation of protein aggregates involves actin and the polarity machinery, 2011.
- [66] L. Luo, Y. J. Liao, L. Y. Jan, and Y. N. Jan. Distinct morphogenetic functions of similar small GTPases: *Drosophila* Drac1 is involved in axonal outgrowth and myoblast fusion. *Genes & development*, 8(15):1787–1802, 1994.
- [67] A. Manz, N. Graber, and H. á. Widmer. Miniaturized total chemical analysis systems: a novel concept for chemical sensing. *Sensors and actuators B: Chemical*, 1(1-6):244–248, 1990.
- [68] P. Medawar. An Unsolved Problem of Biology. *Lewis. London*, 1952.
- [69] F. Meitinger, A. Khmelinskii, S. Morlot, B. Kurtulmus, S. Palani, A. Andres-Pons, B. Hub, M. Knop, G. Charvin, and G. Pereira. A memory system of negative polarity cues prevents replicative aging. *Cell*, 159(5):1056–1069, 2014.
- [70] P. J. Miller and D. I. Johnson. Cdc42p GTPase is involved in controlling polarized cell growth in *Schizosaccharomyces pombe*. *Molecular and cellular biology*, 14(2):1075–1083, 1994.
- [71] Y. Mori, A. Jilkin, and L. Edelstein-Keshet. Wave-pinning and cell polarity from a bistable reaction-diffusion system. *Biophysical journal*, 94(9):3684–3697, 2008.
- [72] R. K. Mortimer and J. R. Johnston. Life span of individual yeast cells. *Nature*, 183(4677):1751–1752, 1959.

- [73] S. Munemitsu, M. A. Innis, R. Clark, F. McCormick, A. Ullrich, and P. Polakis. Molecular cloning and expression of a G25K cDNA, the human homolog of the yeast cell cycle gene CDC42. *Molecular and cellular biology*, 10(11):5977–5982, 1990.
- [74] M. P. Murphy, A. Holmgren, N. G. Larsson, B. Halliwell, C. J. Chang, B. Kalyanaraman, S. G. Rhee, P. J. Thornalley, L. Partridge, D. Gems, T. Nyström, V. Belousov, P. T. Schumacker, and C. C. Winterbourn. Unraveling the biological roles of reactive oxygen species, 2011.
- [75] J. D. Murray. *Mathematical biology II: spatial models and biomedical applications*. Springer New York, 2001.
- [76] J. D. Murray. *Mathematical biology: I. An introduction*, volume 17. Springer Science & Business Media, 2007.
- [77] T. Nyström and B. Liu. Protein quality control in time and space - links to cellular aging. *FEMS Yeast Research*, 2014.
- [78] T. Nyström and B. Liu. The mystery of aging and rejuvenation-a budding topic, 2014.
- [79] P. J. Olver. *Applications of Lie groups to differential equations*, volume 107. Springer Science & Business Media, 2000.
- [80] I. Orlandi, M. Bettiga, L. Alberghina, T. Nyström, and M. Vai. Sir2-dependent asymmetric segregation of damaged proteins in ubp10 null mutants is independent of genomic silencing. *Biochimica et Biophysica Acta (BBA)-Molecular Cell Research*, 1803(5):630–638, 2010.
- [81] M. Otsuji, S. Ishihara, K. Kaibuchi, A. Mochizuki, S. Kuroda, and Others. A mass conserved reaction–diffusion system captures properties of cell polarity. *PLoS computational biology*, 3(6):e108, 2007.
- [82] A. Picca, R. Calvani, M. Bossola, E. Allocca, A. Menghi, V. Pesce, A. M. S. Lezza, R. Bernabei, F. Landi, and E. Marzetti. Update on mitochondria and muscle aging: all wrong roads lead to sarcopenia. *Biological chemistry*, 399(5):421–436, 2018.
- [83] M. Pierre. Global existence in reaction-diffusion systems with control of mass: a survey. *Milan Journal of Mathematics*, 78(2):417–455, 2010.
- [84] H. Pohjanpalo. System identifiability based on the power series expansion of the solution. *Mathematical biosciences*, 41(1-2):21–33, 1978.
- [85] A. Porzoor and I. G. Macreadie. Application of yeast to study the tau and amyloid- β abnormalities of Alzheimer’s disease. *Journal of Alzheimer’s Disease*, 35(2):217–225, 2013.

- [86] S. Ratcliffe. *Oxford essential quotations*. Oxford University Press, 2017.
- [87] A. Rätz and M. Röger. Turing instabilities in a mathematical model for signaling networks. *Journal of mathematical biology*, 65(6-7):1215–1244, 2012.
- [88] A. Rätz and M. Röger. Symmetry breaking in a bulk–surface reaction–diffusion model for signalling networks. *Nonlinearity*, 27(8):1805, 2014.
- [89] S. Rencus-Lazar, Y. DeRowe, H. Adsi, E. Gazit, and D. Laor. Yeast Models for the Study of Amyloid-Associated Disorders and Development of Future Therapy. *Frontiers in Molecular Biosciences*, 6:15, 2019.
- [90] J. A. Rice. *Mathematical statistics and data analysis*. Cengage Learning, 2006.
- [91] M. R. Rose. Evolutionary biology of aging. *Oxford University Press*, 1991.
- [92] B. Sampaio-Marques, C. Felgueiras, A. Silva, M. Rodrigues, S. Tenreiro, V. Franssens, A. S. Reichert, T. F. Outeiro, J. Winderickx, and P. Ludovico. SNCA (α -synuclein)-induced toxicity in yeast cells is dependent on Sir2-mediated mitophagy. *Autophagy*, 8(10):1494–1509, 2012.
- [93] A. J. Santanasto, N. W. Glynn, S. A. Jubrias, K. E. Conley, R. M. Boudreau, F. Amati, D. C. Mackey, E. M. Simonsick, E. S. Strotmeyer, P. M. Coen, B. H. Goodpaster, and A. B. Newman. Skeletal Muscle Mitochondrial Function and Fatigability in Older Adults. *The Journals of Gerontology: Series A*, 70(11):1379–1385, 2014.
- [94] M. Santillán. On the use of the Hill functions in mathematical models of gene regulatory networks. *Mathematical Modelling of Natural Phenomena*, 3(2):85–97, 2008.
- [95] N. S. Savage, A. T. Layton, and D. J. Lew. Mechanistic mathematical model of polarity in yeast. *Molecular biology of the cell*, 23(10):1998–2013, 2012.
- [96] J. Schnakenberg. Simple chemical reaction systems with limit cycle behaviour. *Journal of theoretical biology*, 81(3):389–400, 1979.
- [97] K. L. Schneider, T. Nyström, and P. O. Widlund. Studying spatial protein quality control, proteopathies, and aging using different model misfolding proteins in *S. cerevisiae*. *Frontiers in molecular neuroscience*, 11:249, 2018.
- [98] N. S. Scholes, D. Schnoerr, M. Isalan, and M. P. H. Stumpf. A comprehensive network atlas reveals that Turing patterns are common but not robust. *Cell systems*, 9(3):243–257, 2019.

- [99] A. Sedoglavic. A probabilistic algorithm to test local algebraic observability in polynomial time. *Journal of Symbolic Computation*, 33(5):735–755, 2002.
- [100] K. Shinjo, J. G. Koland, M. J. Hart, V. Narasimhan, D. I. Johnson, T. Evans, and R. A. Cerione. Molecular cloning of the gene for the human placental GTP-binding protein Gp (G25K): identification of this GTP-binding protein as the human homolog of the yeast cell-division-cycle protein CDC42. *Proceedings of the National Academy of Sciences*, 87(24):9853–9857, 1990.
- [101] D. A. Sinclair and L. Guarente. Extrachromosomal rDNA circles - A cause of aging in yeast. *Cell*, 1997.
- [102] R. Spokoini, O. Moldavski, Y. Nahmias, J. L. England, M. Schuldiner, and D. Kaganovich. Confinement to Organelle-Associated Inclusion Structures Mediates Asymmetric Inheritance of Aggregated Protein in Budding Yeast. *Cell Reports*, 2012.
- [103] M. Sunnåker and J. Stelling. Model extension and model selection. In *Uncertainty in Biology*, pages 213–241. Springer, 2016.
- [104] J. Tanevski, L. Todorovski, and S. Džeroski. Combinatorial search for selecting the structure of models of dynamical systems with equation discovery. *Engineering Applications of Artificial Intelligence*, 89:103423, 2020.
- [105] G. Teschl. *Ordinary differential equations and dynamical systems*, volume 140. American Mathematical Soc., 2012.
- [106] P. Tessarz, M. Schwarz, A. Mogk, and B. Bukau. The Yeast AAA+ Chaperone Hsp104 Is Part of a Network That Links the Actin Cytoskeleton with the Inheritance of Damaged Proteins. *Molecular and Cellular Biology*, 2009.
- [107] M. Trogdon, B. Drawert, C. Gomez, S. P. Banavar, T.-M. Yi, O. Campàs, and L. R. Petzold. The effect of cell geometry on polarization in budding yeast. *PLOS Computational Biology*, 14(6):1–22, 2018.
- [108] A. M. Turing. The Chemical Basis of Morphogenesis. *Philosophical transactions of the royal society of London*, 273(641):37–72, 1952.
- [109] J. J. Tyson. Modeling the cell division cycle: cdc2 and cyclin interactions. *Proceedings of the National Academy of Sciences*, 88(16):7328–7332, 1991.

- [110] A. Ugidos, T. Nyström, and A. Caballero. Perspectives on the mitochondrial etiology of replicative aging in yeast. *Experimental Gerontology*, 2010.
- [111] M. Verduyckt, H. Vignaud, T. Bynens, J. den Brande, V. Franssens, C. Cullin, and J. Winderickx. *Yeast as a Model for Alzheimer's Disease: Latest Studies and Advanced Strategies*, pages 197–215. Springer New York, New York, NY, 2016.
- [112] J. D. Watson and F. H. Crick. A Structure for Deoxyribose Nucleic Acid. *Nature*, 171:737–738, apr 1953.
- [113] S. Weinberg. A model of leptons. *Physical review letters*, 19(21):1264, 1967.
- [114] G. Weisgrab, A. Ovsianikov, and P. F. Costa. Functional 3D Printing for Microfluidic Chips. *Advanced Materials Technologies*, 4(10):1900275, 2019.
- [115] L. S. Weisman. Organelles on the move: insights from yeast vacuole inheritance. *Nature reviews Molecular cell biology*, 7(4):243–252, 2006.
- [116] A. Weismann, E. B. Poulton, and E. A. Shipley. Essays upon heredity and kindred biological problems. *Clarendon press*, 1, 1891.
- [117] G. M. Whitesides. The origins and the future of microfluidics. *Nature*, 442(7101):368–373, 2006.
- [118] G. C. Williams. Pleiotropy, Natural Selection, and the Evolution of Senescence. *Evolution*, 1957.
- [119] H. Wu, J. Zhu, Y. Huang, D. Wu, and J. Sun. Microfluidic-based single-cell study: Current status and future perspective. *Molecules*, 23(9):2347, 2018.
- [120] C.-N. Yang and R. L. Mills. Conservation of isotopic spin and isotopic gauge invariance. *Physical review*, 96(1):191, 1954.
- [121] C. Yi, C.-W. Li, S. Ji, and M. Yang. Microfluidics technology for manipulation and analysis of biological cells. *Analytica Chimica Acta*, 560(1-2):1–23, 2006.
- [122] C. Zhou, B. D. Slaughter, J. R. Unruh, A. Eldakak, B. Rubinstein, and R. Li. Motility and segregation of Hsp104-associated protein aggregates in budding yeast. *Cell*, 2011.